Lindblad resonance torques in relativistic discs: II. Computation of resonance strengths

Christopher M. Hirata
Caltech M/C 350-17, Pasadena, California 91125, USA

2 October 2010

ABSTRACT
We present a fully relativistic computation of the torques due to Lindblad resonances from perturbers on circular, equatorial orbits on discs around Schwarzschild and Kerr black holes. The computation proceeds by establishing a relation between the Lindblad torques and the gravitational waveforms emitted by the perturber and a test particle in a slightly eccentric orbit at the radius of the Lindblad resonance. We show that our result reduces to the usual formula for Keplerian discs when taking the nonrelativistic limit. Discs around a black hole possess an $m = 1$ inner Lindblad resonance with no Keplerian analogue; however its strength is very weak even in the moderately relativistic regime ($r/M \sim$ few tens), which is in part due to the partial cancellation of the two leading contributions to the resonant amplitude (the gravitoelectric octupole and gravitomagnetic quadrupole). For equatorial orbits around Kerr black holes, we find that the $m = 1$ ILR strength is enhanced for retrograde spins and suppressed for prograde spins. We also find that the torque associated with the $m \geqslant 2$ inner Lindblad resonances is enhanced relative to the nonrelativistic case; the enhancement is a factor of 2 for the Schwarzschild hole even when the perturber is at a radius of $25M$.

Key words: accretion, accretion discs – relativistic processes – black hole physics.

1 INTRODUCTION

This is the second in a series of two papers devoted to a relativistic computation of torques from an external perturber on a thin disc due to interactions at the Lindblad resonances, i.e. locations in the disc where the orbital frequency Ω and the radial epicyclic frequency κ satisfy $\kappa = \pm m(\Omega - \Omega_{\rm s})$, where $\Omega_{\rm s}$ is the pattern speed of the perturbation. Such resonances have been extensively studied in the nonrelativistic case (e.g. Lynden-Bell & Kalnajs 1972; Goldreich & Tremaine 1978, 1979, 1980; Lin & Papaloizou 1979). In the first paper ("Paper I"), we performed this computation for a general time-stationary, axisymmetric, space-time with an equatorial plane of symmetry and a metric perturbation $h_{\alpha\beta}$ that respects the equatorial symmetry. This paper ("Paper II") completes the evaluation of the Lindblad torque in the case of most interest: the perturbation of the accretion disc surrounding a Schwarzschild or Kerr black hole by a small secondary also orbiting in the equatorial plane. Such computations of the Lindblad resonant strengths may be relevant in the context of electromagnetic counterparts to binary black hole mergers, particularly if an inner disc is involved (Chang et al. 2010). (The more complicated case of perturbations outside of the equatorial plane – as may occur in the case of a merger where the primary

hole is rotating and the secondary is in an inclined orbit – is left to future work.)

The resonant torque formula in Paper I depended on the geodesic properties in the unperturbed spacetime as well as being proportional to the square of the absolute value of the resonant amplitude $\mathcal{S}^{(m)}$, which was a function of the $e^{im\phi}$ Fourier component of the metric perturbation $h_{\alpha\beta}$ and its spatial derivative $h_{\alpha\beta,r}$. The construction of these perturbations generally depends on the solution for the Weyl tensor component ψ_4, which may be solved using a separable wave equation with a source given by the stress-energy tensor associated with the perturber (Teukolsky 1973); and then $h_{\alpha\beta}$ may be obtained by applying a second-order differential operator to a master potential (Chrzanowski 1975), which may be derived from ψ_4 (Wald 1978). Fortunately, for our computations there is a way to circumvent the Chrzanowski (1975) procedure: Paper I showed that the particular combination of metric perturbations we require is related to $\mathcal{P}^{(m)}$, the power delivered to a test particle in a slightly eccentric orbit by the $e^{im\phi}$ component of the perturbation. By replacing the perturber with an equivalent gravitational wave source – either incoming from past null infinity in the case of an inner Lindblad resonance (ILR), or emerging from the past horizon in the case of an outer Lindblad resonance (OLR) – we may equate $\mathcal{P}^{(m)}$ with the power absorbed from the gravitational wave. However, energy is conserved on a

time-independent background metric, and thus $\mathcal{P}^{(m)}$ can be related to the interference between the equivalent gravitational wave representing the perturbation and the gravitational wave emitted by the test particle. This allows us to express the resonant amplitude and hence the resonant torque in terms of the waveforms emitted by the perturber and the test particle (both to future null infinity and into the future horizon), so that standard methods to solve for ψ_4 are sufficient.

The outline of this paper is as follows. In Section 2, we introduce the Kerr metric and review the associated standard notation. Section 3 reviews the geodesics in the Kerr spacetime and their description with action-angle variables, and Section 4 describes the compuation of the perturbation in the Weyl scalar ψ_4; while both of these subjects are standard, there are some differences in our treatment that are particularly suited to the problem at hand, and we make frequent use of intermediate results when taking the non-relativistic limit, so an extended discussion is warranted. Section 5 presents the key new theoretical result of this paper, relating the behaviour of ψ_4 near the horizon and at infinity to the resonant amplitude $\mathcal{S}^{(m)}$. We recompute the resonant amplitudes in the Kepler problem in Section 6, and then proceed to investigate the Lindblad resonances in the Schwarzschild problem in Section 7. Section 8 then considers the Lindblad resonance amplitudes associated with equatorial orbits in the Kerr spacetime. We conclude in Section 9.

2   KERR METRIC AND NOTATION

2.1   The metric and null tetrad

We parameterize the Kerr black hole sequence with the gravitational mass M and the specific angular momentum a. We use relativistic units where the Newtonian gravitational constant and the speed of light are equal to unity. The dimensionless angular momentum is $a_\star \equiv a/M$.

The Kerr metric in Boyer-Lindquist coordinates (Boyer & Lindquist 1967) is

$$
\begin{aligned}
ds^2 &= -\left(1 - \frac{2Mr}{\Sigma}\right) dt^2 - \frac{4Mar}{\Sigma}\sin^2\theta\, dt d\phi \\
&+ \frac{(r^2+a^2)^2 - \Delta a^2 \sin^2\theta}{\Sigma}\sin^2\theta\, d\phi^2 \\
&+ \frac{\Sigma}{\Delta}\, dr^2 + \Sigma\, d\theta^2,
\end{aligned} \tag{1}
$$

where $\Delta \equiv r^2 - 2Mr + a^2$ and $\Sigma \equiv r^2 + a^2 \cos^2\theta$. The contravariant metric coefficients are

$$
g^{tt} = -\frac{(r^2+a^2)^2 - \Delta a^2 \sin^2\theta}{\Delta\Sigma},
$$

$$
g^{t\phi} = -\frac{2aMr}{\Delta\Sigma}, \quad g^{\phi\phi} = \frac{\Delta - a^2\sin^2\theta}{\Delta\Sigma\sin^2\theta}
$$

$$
g^{rr} = \frac{\Delta}{\Sigma}, \quad \text{and} \quad g^{\theta\theta} = \Sigma^{-1}. \tag{2}
$$

The standard Newman-Penrose basis is

$$
\begin{aligned}
\boldsymbol{l} &= \frac{r^2+a^2}{\Delta}\partial_t + \frac{a}{\Delta}\partial_\phi + \partial_r, \\
\boldsymbol{n} &= \frac{\Delta}{2\Sigma}\left(\frac{r^2+a^2}{\Delta}\partial_t + \frac{a}{\Delta}\partial_\phi - \partial_r\right), \\
\boldsymbol{m} &= \frac{ia\sin\theta\,\partial_t + \partial_\theta + i\csc\theta\,\partial_\phi}{\sqrt{2}\,(r + ia\cos\theta)}, \text{ and} \\
\bar{\boldsymbol{m}} &= \frac{-ia\sin\theta\,\partial_t + \partial_\theta - i\csc\theta\,\partial_\phi}{\sqrt{2}\,(r - ia\cos\theta)}.
\end{aligned} \tag{3}
$$

Expressions involving $\boldsymbol{m}$ can be simplified if we use

$$
\rho = \frac{-1}{r - ia\cos\theta} \quad \text{and} \quad \bar{\rho} = \frac{-1}{r + ia\cos\theta}, \tag{4}
$$

which satisfy $\rho\bar{\rho} = \Sigma^{-1}$. The Weyl scalar ψ_4 used to describe the emitted gravitational waveform is

$$
\psi_4 = -C_{\alpha\beta\gamma\delta}n^\alpha\bar{m}^\beta n^\gamma \bar{m}^\delta = -R_{\alpha\beta\gamma\delta}n^\alpha\bar{m}^\beta n^\gamma \bar{m}^\delta, \tag{5}
$$

where $C_{\alpha\beta\gamma\delta}$ is the Weyl tensor, and the equivalence to the component formed from the Riemann tensor $R_{\alpha\beta\gamma\delta}$ is due to the Newman-Penrose basis conditions.

The horizons of the black hole are at radial coordinate

$$
r_{\mathrm{h}\pm} = M \pm \sqrt{M^2 - a^2}. \tag{6}
$$

Particles very close to the horizon ($r - r_{\mathrm{h}+} \to 0^+$) rotate at a pattern speed of the hole's angular velocity:

$$
\Omega_{\mathrm{H}} = \frac{a}{2Mr_{\mathrm{h}+}} = \frac{a}{r_{\mathrm{h}+}^2 + a^2} = \frac{1 - \sqrt{1 - a_\star^2}}{2a_\star M}. \tag{7}
$$

Note that for real coordinates, $\bar{\boldsymbol{m}} = \boldsymbol{m}^*$ and $\bar{\rho} = \rho^*$, where * denotes the complex conjugate; however we will occasionally analytically continue r to complex values, in which case the barred quantities are not the complex conjugates of the unbarred quantities: $\bar{\rho}(r,\theta) = \rho^*(r^*,\theta^*) \neq \rho^*(r,\theta)$.

Finally, we define

$$
K \equiv \omega(r^2 + a^2) - am \tag{8}
$$

and use the angular operator

$$
\mathbb{L}_n^\dagger \equiv \partial_\theta - m\csc\theta + a\omega\sin\theta + n\cot\theta. \tag{9}
$$

2.2   Notation in related works

Our notation appears to be common in the literature but other examples can be found.

• We are consistent with the metric and (where applicable) null tetrad used in the standard general relativity text by Wald (1984). Misner et al. (1973) use "ρ^2" to denote our Σ, and do not fix a normalization for the principal null vectors.

• Chandrasekhar (1992) uses the $+ - - -$ signature, and uses "ρ^2" to denote our Σ; "φ" to denote our ϕ; "Σ^2" to denote our $(r^2+a^2)^2 - \Delta a^2 \sin^2\theta$; and δ to denote our $\sin^2\theta$. For the perturbations, Chandrasekhar (1992) denotes the frequency by $-\sigma^+$, and uses the opposite sign of K. Additionally, our ρ and $\bar{\rho}$ are denoted by $-\bar{\rho}^{-1*}$ and $-\bar{\rho}^{-1}$, respectively. However, the null tetrad and the operators $\mathbb{L}_n$ and $\mathbb{L}_n^\dagger$ are the same.

3 TIMELIKE GEODESICS IN KERR

We utilize the Hamiltonian formulation of the equations of motion for a particle. As is well-known, the action for a particle of mass μ is $S = -\mu \int d\tau$, where τ is the proper time along the particle trajectory. For our purposes, the fastest route to the torque formula is *not* to use the covariant representation of the action but rather to explicitly parameterize the particle's trajectory using the coordinate time t, which is always possible outside the outer horizon. This method, which explicitly keeps only the 3 physical degrees of freedom, is best suited to a perturbation analysis.

As in Newtonian perturbation theory analyses, it is most convenient to work with action-angle variables, using the 3+1 version of the Hamiltonian that retains no gauge freedom associated with the particle trajectory. Hinderer & Flanagan (2008) constructed a set of action-angle variables in which the particle's trajectory is parameterized by *proper* time τ, and t is promoted to a dynamical variable (with conjugate momentum $p_t = -\mu\mathcal{E}$). Their actions (J_r, J_θ, J_ϕ) are equal to ours, since the momenta are the same, however the angle variables are different since ours advance at uniform rate with respect to coordinate time and theirs advance at a uniform rate with respect to proper time. Thus the Fourier decompositions are also different. Other works that have constructed the Hamiltonian for geodesic motion in 4-dimensional space have projected the motion into the 3 physical degrees of freedom (Schmidt 2002), but appear not to have constructed the full transformation from action-angle variables to the familiar spatial coordinates and momenta, which we will need to complete here. Flanagan & Hinderer (2010) considered resonances in inspiralling black hole binaries, but parameterize their trajectory in terms of the "Mino time" $\lambda = \int d\tau/\Sigma$ (Mino 2003; Drasco et al. 2005). This again means that they have an additional conjugate variable pair not present in our treatment, and that their angle variables advance at a constant rate as measured by λ rather than by t.

3.1 Hamiltonian and constants of the motion

The trajectory of a massive particle can be followed by parameterizing the trajectory $x^i(t)$ where $x^i \in \{r, \theta, \phi\}$, and using the action $S = -\tau$. This results in the Hamiltonian $H = -p_t$, where p_t is determined from the p_i via the mass-shell condition (Paper I):

$$H(t, x^i, p_i) = \frac{g^{ti}p_i - \sqrt{(g^{ti}p_i)^2 - g^{tt}g^{ij}p_ip_j - \mu^2 g^{tt}}}{g^{tt}}. \quad (10)$$

The timelike geodesics in the Kerr metric are characterized by three constants: the energy per unit mass $\mathcal{E} = -p_t/\mu = -u_t$; the angular momentum around the symmetry axis per unit mass, $\mathcal{L} = p_\phi/\mu = u_\phi$; and the Carter constant,

$$\mathcal{Q} = 2\Sigma(\boldsymbol{u} \cdot \boldsymbol{l})(\boldsymbol{u} \cdot \boldsymbol{n}) - r^2 - (\mathcal{L} - a\mathcal{E})^2, \quad (11)$$

which may also be expressed using

$$\mathcal{K} = \mathcal{Q} + (\mathcal{L} - a\mathcal{E})^2. \quad (12)$$

Given the three constants of the motion $\{\mathcal{E}, \mathcal{Q}, \mathcal{L}\}$, it is possible to obtain the momenta when the particle passes through any spatial position (r, θ, ϕ). Specifically, we always

have eastward momentum $u_\phi = \mathcal{L}$. The southward momentum given by Eq. (7.164) of Chandrasekhar (1992),

$$u_\theta^2 = \mathcal{Q} - a^2(1 - \mathcal{E}^2)\cos^2\theta - \mathcal{L}^2\cot^2\theta, \quad (13)$$

and the radial momentum by Eq. (7.160) of Chandrasekhar (1992),

$$\Delta^2 u_r^2 = [(r^2 + a^2)\mathcal{E} - a\mathcal{L}]^2 - \Delta(r^2 + \mathcal{K}). \quad (14)$$

3.2 Actions in terms of the energy, Carter constant, and angular momentum

It is useful in integrable problems to define the action-angle variables. We begin by considering the actions corresponding to the r, θ, and ϕ loops around the invariant torus corresponding to a set of constants $\{\mathcal{E}, \mathcal{Q}, \mathcal{L}\}$. The ϕ-direction is the easiest: the action is

$$J_\phi = \frac{1}{2\pi} \oint_0^{2\pi} p_\phi \, d\phi = p_\phi = \mu\mathcal{L}. \quad (15)$$

We define the notation $\tilde{J}_\phi \equiv J_\phi/\mu = \mathcal{L}$.

For the θ-direction, we use Eq. (13), which defines a loop in the (θ, u_θ)-plane. Its area,

$$\tilde{J}_\theta = \frac{1}{2\pi} \oint u_\theta \, d\theta, \quad (16)$$

involves an elliptic function, which however is most easily evaluated by numerical integration. It is convenient to switch to the variable $z = \cos\theta$, in which case we find

$$(1 - z^2)u_\theta^2 = \mathcal{Q}(1 - z^2) - a^2(1 - \mathcal{E}^2)z^2(1 - z^2) - \mathcal{L}^2z^2. \quad (17)$$

The turning points are found at the zeroes of the right-hand side, which is quadratic in z^2. These zeroes are $z^2 = z_\pm^2$; inspection of the signs at $z^2 \in \{0, 1, \infty\}$ shows that they have the ordering $0 < z_-^2 < 1 < z_+^2$. These zeroes can then be found by bisection.

We may then write, recalling that via change of variables $u_z = (1 - z^2)^{-1/2}u_\theta$,

$$u_z^2 = \mathcal{Q}(1 - z^2)^{-2}\left(1 - \frac{z^2}{z_-^2}\right)\left(1 - \frac{z^2}{z_+^2}\right). \quad (18)$$

The action is then

$$\tilde{J}_\theta = \frac{\mathcal{Q}^{1/2}}{2\pi} \oint \sqrt{\left(1 - \frac{z^2}{z_-^2}\right)\left(1 - \frac{z^2}{z_+^2}\right)} \frac{dz}{1 - z^2}. \quad (19)$$

We have solved this integral with the substitution $z = z_-\sin(\frac{1}{2}\pi\tanh\xi)$, where the full integral is given by 4 times the integral $\int_0^\infty d\xi$. Written in terms of ξ, the integrand is smooth, even, and decays exponentially at large ξ. Summation of the integrand in ξ at points $(n + \frac{1}{2})\Delta\xi$ thus enables evaluation of the integral with exponentially small error as $\Delta\xi \to 0^+$ and $N\Delta\xi \to \infty$ (where N is the number of points).

For the r-direction, Eq. (14) defines a loop in the (r, u_r)-plane, and one may again find the area

$$\tilde{J}_r = \frac{1}{2\pi} \oint u_r \, dr. \quad (20)$$

A practical solution for $\tilde{J}_r$ is to find the turning points r_- and r_+ by solving the quartic equation $\Delta^2 u_r^2 = 0$ for r,

4   *Hirata*

Eq. (14).[1] Then a substitution of the form

$$r = \frac{r_+ + r_-}{2} - \frac{r_+ - r_-}{2}\tanh\beta \qquad (21)$$

enables one to turn the integral into one over $-\infty < \beta < \infty$ (multiplied by 2 to get the inward leg of the trajectory), where the integrand is analytic in the vicinity of the real β-axis and declines exponentially as $\beta \to \pm\infty$; it may thus be evaluated by the simple method of summing the integrand at equally spaced abscissae β.

A problem one may encounter is that there is only a finite range of energies $[\mathcal{E}_{\min}(\mathcal{L}, Q), \mathcal{E}_{\max}(\mathcal{L}, Q)]$ over which bound orbits can exist. The sign pattern of the extrema can be used to distinguish the $\mathcal{E} < \mathcal{E}_{\min}$ versus $\mathcal{E} > \mathcal{E}_{\max}$ cases.

3.3 Geodesic properties

For a given value of the actions $(\tilde{J}_r, \tilde{J}_\theta, \tilde{J}_\phi)$, one may obtain the constants of the motion $\{\mathcal{E}, Q, \mathcal{L}\}$ by inverting the equation for the actions in terms of the constants of the motion. The determination of $\mathcal{L} = \tilde{J}_\phi$ is trivial. The determination of $\mathcal{E}$ and Q is harder, requiring the solution of a nonlinear system of two equations; we solve these iteratively by first writing a function to obtain $\mathcal{E}(\tilde{J}_r, Q, \tilde{J}_\phi)$ by bisection solution of $\tilde{J}_r(\mathcal{E}, Q, \mathcal{L}) = \tilde{J}_r$; and then writing a function to adjust Q (again by a bisection search) until we find the desired $\tilde{J}_\theta$.

We will often need the 3×3 matrix of partial derivatives

$$\mathsf{M} = \begin{pmatrix} \frac{\partial\mathcal{E}}{\partial\tilde{J}_r} & \frac{\partial Q}{\partial\tilde{J}_r} & \frac{\partial\mathcal{L}}{\partial\tilde{J}_r} \\ \frac{\partial\mathcal{E}}{\partial\tilde{J}_\theta} & \frac{\partial Q}{\partial\tilde{J}_\theta} & \frac{\partial\mathcal{L}}{\partial\tilde{J}_\theta} \\ \frac{\partial\mathcal{E}}{\partial\tilde{J}_\phi} & \frac{\partial Q}{\partial\tilde{J}_\phi} & \frac{\partial\mathcal{L}}{\partial\tilde{J}_\phi} \end{pmatrix}. \qquad (22)$$

The last column of M is simply $(0,0,1)^{\mathrm{T}}$. The first column is notable for being the vector of fundamental angular frequencies corresponding to the r, θ, and ϕ directions on the torus, $(\Omega_r, \Omega_\theta, \Omega_\phi)^{\mathrm{T}}$.

It is possible to obtain M by numerical differentiation, but it is more accurate to obtain its inverse M^{-1} by differentiating the actions with respect to $(\mathcal{E}, Q, \mathcal{L})$. The last column (the vector of partial derivatives of $\tilde{J}_\phi$) is simply $(0,0,1)^{\mathrm{T}}$. The second column (the vector of partial derivatives of $\tilde{J}_\theta$) can be obtained using the relation

$$\frac{\partial J_\theta}{\partial A} = \frac{1}{2\pi}\oint \frac{\partial u_z}{\partial A}\bigg|_z \, dz = \frac{1}{4\pi}\oint \frac{\partial(u_z^2)}{\partial A}\bigg|_z \frac{dz}{u_z}, \qquad (23)$$

where $A \in \{\mathcal{E}, Q, \mathcal{L}\}$ we have used the fact that $u_z \to 0$ at the turning points to set to zero terms associated with changes in $z_{\min,\max}$. The explicit expressions are

$$u_z = \frac{\left[Q(1-z^2) - a^2(1-\mathcal{E}^2)z^2(1-z^2) - \mathcal{L}^2 z^2\right]^{1/2}}{1-z^2}, \quad (24)$$

with derivatives

$$\frac{\partial(u_z^2)}{\partial\mathcal{E}} = \frac{2a^2\mathcal{E}z^2}{1-z^2},$$

$$\frac{\partial(u_z^2)}{\partial Q} = \frac{1}{1-z^2}, \quad \text{and}$$

$$\frac{\partial(u_z^2)}{\partial\mathcal{L}} = -\frac{2\mathcal{L}z^2}{(1-z^2)^2}. \qquad (25)$$

Near the turning points or for low inclinations, u_z becomes small, which is an issue since it is in the denominator of Eq. (23). We thus set $z = z_-\tanh\alpha$, perform the integral for $0 < \alpha < \infty$, and then multiply by 4 to get the whole cycle; using Eq. (18) this gives

$$\frac{dz}{u_z} = \frac{z_-}{Q^{1/2}} \frac{1-z^2}{\sqrt{1-z^2/z_+^2}}\operatorname{sech}\alpha \, d\alpha. \qquad (26)$$

For large inclinations, $z_-/Q^{1/2}$ may be obtained directly; for small inclinations ($z_- < 10^{-8}$), the equatorial limit may be used,

$$\lim_{Q\to 0^+} \frac{z_-}{Q^{1/2}} = \frac{1}{\sqrt{\mathcal{L}^2 + a^2(1-\mathcal{E}^2)}}. \qquad (27)$$

A similar approach works for the derivatives of the radial action. In this case, we need

$$\frac{\partial J_r}{\partial A} = \frac{1}{4\pi}\oint \frac{\partial(u_r^2)}{\partial A}\bigg|_r \frac{dr}{u_r}. \qquad (28)$$

This time, the desired substitution is Eq. (21), with which we find

$$\frac{dr}{u_r} = \frac{(r_+ - r_-)\Delta}{2\sqrt{P(r)}}\operatorname{sech}^2\beta \, d\beta, \qquad (29)$$

where $P(r)$ is the polynomial on the right-hand side of Eq. (14). If we factor the polynomial as

$$P(r) = -(1-\mathcal{E}^2)(r-r'_-)(r-r'_+)(r-r_-)(r-r_+), \quad (30)$$

where $r_\pm$ and $r'_\pm$ are the four roots,[2] then we may simplify this to

$$\frac{dr}{u_r} = \frac{\Delta}{\sqrt{(1-\mathcal{E}^2)(r-r'_-)(r-r'_+)}}\operatorname{sech}\beta \, d\beta. \qquad (31)$$

The derivatives are:

$$\frac{\partial(u_r^2)}{\partial\mathcal{E}} = \frac{2[(r^2+a^2)\mathcal{E} - a\mathcal{L}](r^2+a^2)}{\Delta^2} + \frac{2a(\mathcal{L}-a\mathcal{E})}{\Delta},$$

$$\frac{\partial(u_r^2)}{\partial Q} = -\frac{1}{\Delta}, \quad \text{and}$$

$$\frac{\partial(u_r^2)}{\partial\mathcal{L}} = \frac{-2a[(r^2+a^2)\mathcal{E} - a\mathcal{L}]}{\Delta^2} - \frac{2(\mathcal{L}-a\mathcal{E})}{\Delta}. \qquad (32)$$

3.4 Particle position and momentum in terms of the action-angle variables

In perturbation theory it is critical to be able to obtain the particle's phase space location (x^i, p_i) in terms of the action-angle variables $(\tilde{J}_i, \psi^i)$. The generic procedure to do

---

[1] We solve the equation by first finding the inflection points (via a quadratic equation) and then using the bisection method to find the extrema. Finally a further bisection gives the roots. The sign pattern of the extrema determines whether there are 1 or 3 roots outside the outer horizon; stable bound orbits require 3 roots.

[2] These are all real in the case of stable orbits since $P(r)$ is negative at $r = 0$, positive at the outer horizon $r = r_{\mathrm{h}+}$, and then has 3 roots outside the outer horizon.

this is as follows. First, for a given $\{\tilde{J}_i\}$, we identify the constants of the motion $\{\mathcal{E}, \mathcal{Q}, \mathcal{L}\}$ on the corresponding torus. These three actions mutually commute: $\{J_i, J_j\}_P = 0$, where $\{,\}_P$ denotes the Poisson bracket. Second, we must construct the angle variables. For actual numerical computation, the method of choice is to use the direct conditions to construct the mapping of $(J_i, \psi^i) \rightarrow (x^i, p_i)$, which will depend on the (unknown) origin of the angle coordinates $\psi = (0,0,0)$ on each torus; and we will find a valid origin by inspection.

We first use the direct conditions (e.g. Goldstein et al. 2002, Eq. 9.48) to write a system of differential equations for x^i and p_i as functions of the angles for fixed $\boldsymbol{J}$:

$$\frac{\partial x^i}{\partial \psi^j}\bigg|_{\tilde{J}_k} = \frac{\partial \tilde{J}_j}{\partial u_i}\bigg|_{x^k} \text{ and } \frac{\partial u_i}{\partial \psi^j}\bigg|_{\tilde{J}_k} = -\frac{\partial \tilde{J}_j}{\partial x^i}\bigg|_{u_k}. \quad (33)$$

These equations can be re-written in terms of derivatives of constants of the motion,

$$\frac{\partial x^i}{\partial \psi^j}\bigg|_{\tilde{J}_k} = \sum_{A \in \{\mathcal{E},\mathcal{Q},\mathcal{L}\}} [\mathbf{M}^{-1}]_{A,j} \frac{\partial A}{\partial u_i}\bigg|_{x^k}, \quad (34)$$

and similarly for u_i. These equations define a solution for ψ, except that we must choose an origin $\psi = 0$ on each torus; thus all possible solutions differ by a transformation of the form $\psi^i \rightarrow \psi^i + f^i(\tilde{\boldsymbol{J}})$.

Our next step is to determine an appropriate choice of origin, i.e. the 3-dimensional submanifold of phase space corresponding to $\psi = \mathbf{0}$. All valid choices of angle variables correspond to some origin (and are related to each other by simple phase-shifts of the angle variables on each torus), but in multiple dimensions not all origins correspond to valid angle variables.[3] Arnold (1978, §50C) shows that a (locally) valid choice of origin is $Q^i =$ constant, where (Q^i, P_i) are a set of canonical coordinates.[4] We could thus choose a particular value of (r, θ, ϕ) as our origin; but this would not be applicable to all orbits since there is no value of r that all orbits cross. We prefer to choose fixed (p_r, θ, ϕ), which is also valid since Hamiltonian mechanics does not distinguish between the position and momentum variables[5]; we take $p_r = 0$, $\theta = \pi/2$, and $\phi = 0$.

It is then necessary only to apply certain inequalities so that each torus intersects the $\psi = \mathbf{0}$ manifold once and the angle coordinates are defined globally on each torus; we take $\partial H/\partial r < 0$ and $p_\theta < 0$. This corresponds to the point of pericentre and ascending node at zero longitude, i.e.

$$x^i = \left(r_-, \frac{\pi}{2}, 0\right) \text{ and } u_i = \left(0, -\mathcal{Q}^{1/2}, \mathcal{L}\right). \quad (35)$$

Starting from $\psi = (0,0,0)$, we may use Eq. (34) to evolve the particle to any chosen angle coordinates. Since the construction of the torus integrates over no more than 1

cycle, even a simple integrator is sufficient (we use the 4th order explicit Runge-Kutta method).

We finally need the formulas for the partial derivatives of $\mathcal{E}$, $\mathcal{Q}$, and $\mathcal{L}$ with respect to (x^i, p_i). For $\mathcal{E}$, this is simple: the partial derivatives represent the Hamiltonian flow,

$$\frac{\partial \mathcal{E}}{\partial p_i} = \frac{\partial H}{\partial p_i} = \dot{x}^i = \frac{u^i}{u^t}, \quad (36)$$

where u^t is determined from the mass-shell condition $\boldsymbol{u} \cdot \boldsymbol{u} = -1$. The variation of the momentum can be determined from the conserved quantities, e.g. by taking the t-derivative of Eq. (13),

$$2u_\theta \dot{u}_\theta = [2a^2(1-\mathcal{E}^2)\cos\theta\sin\theta + 2\mathcal{L}^2\cot\theta\csc^2\theta]\dot{\theta}; \quad (37)$$

using that $\dot{\theta} = u^\theta/u^t = u_\theta/(\Sigma u^t)$, we find

$$-\frac{\partial \mathcal{E}}{\partial \theta} = \dot{u}_\theta = \frac{a^2(1-\mathcal{E}^2)\cos\theta\sin\theta + \mathcal{L}^2\cot\theta\csc^2\theta}{\Sigma u^t}. \quad (38)$$

We also know trivially that

$$-\frac{\partial \mathcal{E}}{\partial \phi} = 0. \quad (39)$$

Finally, taking $\frac{1}{2}$ of the t-derivative of Eq. (14) gives

$$\Delta^2 u_r \dot{u}_r + 2(r-M)\Delta u_r^2 \dot{r} = 2[(r^2+a^2)\mathcal{E} - a\mathcal{L}]r\mathcal{E}\dot{r} - r\Delta\dot{r} \\ -(r-M)(r^2+K)\dot{r}. \quad (40)$$

One then uses $\dot{r} = u^r/u^t = \Delta u_r/(\Sigma u^t)$ to obtain:

$$-\frac{\partial \mathcal{E}}{\partial r} = \dot{u}_r = \frac{2[(r^2+a^2)\mathcal{E} - a\mathcal{L}]r\mathcal{E}}{\Delta\Sigma u^t} - \frac{r}{\Sigma u^t} \\ -\frac{(r-M)(r^2+K)}{\Delta\Sigma u^t} - \frac{2(r-M)}{\Sigma u^t}u_r^2. \quad (41)$$

We may find the derivatives of $\mathcal{Q}$ by taking the differential of Eq. (13):

$$d\mathcal{Q} = 2[u_\theta \, du_\theta - a^2(1-\mathcal{E}^2)\cos\theta\sin\theta \, d\theta - a^2\mathcal{E}\cos^2\theta \, d\mathcal{E} \\ +\mathcal{L}\cot^2\theta \, d\mathcal{L} - \mathcal{L}^2\cot\theta\csc^2\theta \, d\theta]. \quad (42)$$

Recalling that $\mathcal{L} = u_\phi$, and using the aforementioned rules to obtain the partial derivatives of $\mathcal{E}$, we may find $\partial\mathcal{Q}/\partial x^i$ and $\partial\mathcal{Q}/\partial p_i$.

This argument allows us to take any action-angle variables (ψ^i, J_i) and construct the usual coordinates (x^i, p_i). We have not implemented an inverse function $(x^i, p_i) \rightarrow (\psi^i, J_i)$ since it is not required for this work, although we do not expect it to present any special difficulty.

4 GRAVITATIONAL PERTURBATIONS

We next describe the solution of the equations for the Weyl tensor component ψ_4 given the particle trajectory. The approach is to use the separability of the equations to write

$$\psi_4(t, r\theta, \phi) = \rho^4 \sum_{\ell m} \int_{-\infty}^{\infty} \mathcal{R}_{\ell m\omega}(r) S_{\ell,m}^{-2,\chi}(\theta) e^{i(m\phi-\omega t)} \frac{d\omega}{2\pi}, \quad (43)$$

where the radial function $R_{\ell m\omega}(r)$ satisfies a homogeneous equation (in vacuum) or an inhomogeneous equation (in the present case, with source). The separated equation and the behaviour of the radial solutions were considered by Teukolsky (1973); we will thus describe in detail here only the aspects that are required for either our numerical techniques or for the treatment of the Keplerian limit.

---

[3] A trivial way to see this is to note that the direct conditions show a transformation $\psi^i \rightarrow \psi^i + f^i(\boldsymbol{J})$ to be canonical if and only if the 3×3 matrix $\partial f^i/\partial J_j$ is symmetric, i.e. if f is derivable from a potential: $f^i(\boldsymbol{J}) = \partial\Phi/\partial J_i$ for some $\Phi(\boldsymbol{J})$.
[4] The construction in Arnold (1978) technically shows that the generating function for the transformation $(Q^i, P_i) \rightarrow (\psi^i, J_i)$ vanishes at the chosen origin; but inspection shows that $\psi = \mathbf{0}$ there as well.
[5] This argument is equivalent to applying first a canonical transformation $Q^r = p_r$, $P_r = -r$, and then the construction in Arnold (1978).

4.1 Angular eigenfunctions

We are interested here in the solutions of the latitude eigenfunctions $S_{\ell,m}^{s,\chi}(\theta)$ that satisfy the eigenvalue equation (Hughes 2000, Appendix A)

$$
\begin{aligned}
-\mathcal{E}_{\ell,m}^s S_{\ell,m}^{s,\chi}(\theta) \;=\;& \partial_\theta^2 S_{\ell,m}^{s,\chi}(\theta) + \cot\theta\,\partial_\theta S_{\ell,m}^{s,\chi}(\theta) \\
&+ \chi^2\cos^2\theta\, S_{\ell,m}^{s,\chi}(\theta) - 2s\chi\cos\theta\, S_{\ell,m}^{s,\chi}(\theta) \\
&- \frac{m^2 + 2ms\cos\theta + s^2}{\sin^2\theta} S_{\ell,m}^{s,\chi}(\theta).
\end{aligned}
\tag{44}
$$

Here $S_{\ell,m}^{\chi}(\theta)$ denotes the values at $\phi = 0$; we understand that

$$
S_{\ell,m}^{\chi}(\theta,\phi) = S_{\ell,m}^{\chi}(\theta)\mathrm{e}^{\mathrm{i}m\phi}.
\tag{45}
$$

For gravitational wave problems using the gauge-invariant Weyl tensor component ψ_4 one requires the $s = -2$ harmonics with $\chi \equiv a\omega$. The vertical quantum number ℓ begins at $\ell_{\min} = \max(|m|,|s|)$ by convention. The solution method is standard and is described in Appendix A.

4.2 The radial equation: homogeneous piece

The radial equation can be written as, suppressing the indices $\ell m\omega$,

$$
\Delta^2 \frac{\mathrm{d}}{\mathrm{d}r}\left(\Delta^{-1}\frac{\mathrm{d}\mathcal{R}}{\mathrm{d}r}\right) - V\mathcal{R} = -\mathcal{T},
\tag{46}
$$

where $\mathcal{T}$ is a source term to be described later and the potential is (Teukolsky 1973, Eq. 4.9)

$$
V(r) = \frac{-K^2 - 4\mathrm{i}(r-M)K}{\Delta} + 8\mathrm{i}\omega r + \mathcal{E} - 2am\omega + a^2\omega^2 - 2.
\tag{47}
$$

We consider first the solution of the source-free homogeneous equation subject to either the boundary condition of a purely ingoing gravitational wave at the horizon $r = r_{\mathrm{h}+}$, or a purely outgoing wave at $r = \infty$. The matching condition in between in the presence of sources will be considered next.

It is standard to use the radial coordinate $r_\star$ defined by

$$
\frac{\mathrm{d}r_\star}{\mathrm{d}r} = \frac{r^2 + a^2}{\Delta},
\tag{48}
$$

or explicitly (e.g. Hughes 2000)

$$
r_\star = r + \frac{r_{\mathrm{h}+}}{\sqrt{1-a_\star^2}}\ln\frac{r-r_{\mathrm{h}+}}{2M} + \frac{r_{\mathrm{h}-}}{\sqrt{1-a_\star^2}}\ln\frac{r-r_{\mathrm{h}-}}{2M}.
\tag{49}
$$

In the $r_\star$ coordinate, the radial equation becomes

$$
\frac{(r^2+a^2)^2}{\Delta}\frac{\mathrm{d}^2\mathcal{R}}{\mathrm{d}r_\star^2} + 2\frac{r\Delta - 2(r-M)(r^2+a^2)}{\Delta}\frac{\mathrm{d}\mathcal{R}}{\mathrm{d}r_\star} - V\mathcal{R} = 0.
\tag{50}
$$

4.2.1 Inner solution

We consider the inner region first. In this region, as $r_\star \to -\infty$ and $r \to r_{\mathrm{h}+}$, we have

$$
r - r_{\mathrm{h}+} \approx 2M\exp\left[\frac{\sqrt{1-a_\star^2}}{r_{\mathrm{h}+}}(r_\star - r_{\mathrm{h}+})\right].
\tag{51}
$$

Then since $\Delta = (r-r_{\mathrm{h}-})(r-r_{\mathrm{h}+})$, we have $\Delta \propto \mathrm{e}^{\Gamma r_\star}$, where

$$
\Gamma = \frac{\sqrt{1-a_\star^2}}{r_{\mathrm{h}+}} = \frac{2\sqrt{M^2-a^2}}{r_{\mathrm{h}+}^2 + a^2},
\tag{52}
$$

where in the last equality we have used the root equation for the horizon, $r_{\mathrm{h}+}^2 - 2Mr_{\mathrm{h}+} + a^2 = 0$. We further see that

$$
\lim_{r\to r_{\mathrm{h}+}} \frac{2(r-M)}{r^2+a^2} = \Gamma
\tag{53}
$$

and

$$
\lim_{r\to r_{\mathrm{h}+}} \frac{K}{r^2+a^2} = \omega - m\Omega_{\mathrm{H}} \equiv \varpi.
\tag{54}
$$

Then in the limit $r_\star \to -\infty$, the differential equation becomes

$$
\frac{\mathrm{d}^2R}{\mathrm{d}r_\star^2} - 2\Gamma\frac{\mathrm{d}\mathcal{R}}{\mathrm{d}r_\star} + (\varpi^2 + 2\mathrm{i}\Gamma\varpi)\mathcal{R} = 0;
\tag{55}
$$

the two solutions are then exponentials,

$$
\mathcal{R}_1(r_\star) \propto \mathrm{e}^{(-\mathrm{i}\varpi+2\Gamma)r_\star} \quad\text{and}\quad \mathcal{R}_2(r_\star) = \mathrm{e}^{\mathrm{i}\varpi r_\star}.
\tag{56}
$$

Teukolsky (1973) obtained these solutions and found that $\mathcal{R}_1$ corresponds to the ingoing wave and $\mathcal{R}_2$ to the outgoing wave. Thus, interior to any matter sources, the physical solution must be that which matches to $\alpha_1\mathcal{R}_1$, where α_1 is some (possibly complex) constant. Since $\Gamma > 0$ and $\mathcal{R}_1$ increases exponentially outward relative to $\mathcal{R}_2$, no numerical difficulty arises in starting at some large negative value of $r_\star$, setting

$$
\mathcal{R}_1 = \Delta^2\mathrm{e}^{-\mathrm{i}\varpi r_\star} \quad\text{and}\quad \frac{\mathrm{d}\mathcal{R}_1}{\mathrm{d}r_\star} = (-\mathrm{i}\varpi + 2\Gamma)\Delta^2\mathrm{e}^{-\mathrm{i}\varpi r_\star},
\tag{57}
$$

and integrating outward with a standard (RK4) integrator.

4.2.2 Outer solution

The radial equation in the outer region $(r_\star \to \infty)$ is not so well behaved. In this limit, we find

$$
\frac{\Delta}{(r^2+a^2)^2}V \to -\omega^2 + 4\mathrm{i}\omega r_\star^{-1} + \mathcal{O}(r_\star^{-2}).
\tag{58}
$$

and the radial equation becomes (keeping the leading-order terms in $r_\star^{-1}$)

$$
\frac{\mathrm{d}^2\mathcal{R}}{\mathrm{d}r_\star^2} - \frac{2}{r_\star}\frac{\mathrm{d}\mathcal{R}}{\mathrm{d}r_\star} + \left(\omega^2 - \frac{4\mathrm{i}\omega}{r_\star}\right)\mathcal{R} = 0.
\tag{59}
$$

This may be turned into a quadratic equation for the WKB wave number k with the replacement $\mathrm{d}/\mathrm{d}r_\star \to \mathrm{i}k$; the solutions, to lowest order in $r_\star^{-1}$, are

$$
k_3 = \omega - \frac{3\mathrm{i}}{r_\star} \quad\text{and}\quad k_4 = -\omega + \frac{\mathrm{i}}{r_\star}.
\tag{60}
$$

This implies an imaginary logarithmic divergence of the phases, or equivalently a power-law behavior of the real parts of the solutions at $r_\star \to \infty$,

$$
\mathcal{R}_3 \to r_\star^3\mathrm{e}^{\mathrm{i}\omega r_\star} \quad\text{and}\quad \mathcal{R}_4 \to r_\star^{-1}\mathrm{e}^{-\mathrm{i}\omega r_\star}.
\tag{61}
$$

Here $\mathcal{R}_3$ corresponds to a purely outgoing wave and is the physical solution in problems where there is no incident gravitational radiation. ($\mathcal{R}_4$ corresponds to a purely ingoing wave.) However, as noted by Press & Teukolsky (1973), if one integrates from large to small $r_\star$, the $\mathcal{R}_4$ solution grows relative to $\mathcal{R}_3$, so it quickly begins to dominate. Several solutions to this problem exist in the literature, such as using a highly accurate integrator such that the $\mathcal{R}_4$ solution remains subdominant (Press & Teukolsky 1973); or evolving a linear combination of $\mathcal{R}$ and $\mathrm{d}\mathcal{R}/\mathrm{d}r_\star$ that eliminates the

subdominance of $\mathcal{R}_4$ as $r \to \infty$ (Press & Teukolsky 1973) or lacks the long-range imaginary part of the potential that causes the divergence (Sasaki & Nakamura 1982a,b).

An alternative, which we use here, is to note that Eq. (46) is a regular linear ODE with analytic coefficients except at $r \in \{r_{\mathrm{h}-}, r_{\mathrm{h}+}, \infty\}$. Therefore, if we desire $\mathcal{R}_3$ and $\mathrm{d}\mathcal{R}_3/\mathrm{d}r$ at any real value of $r > r_{\mathrm{h}+}$, it is permissible to integrate the ODE on any convenient path through the complex plane. We note further that if $\Re r$ is large, then while $|\mathcal{R}_3|$ grows more rapidly than $|\mathcal{R}_4|$ on the *real axis*, if $\Im r$ is allowed to be positive then $|\mathcal{R}_4|$ is exponentially enhanced relative to $|\mathcal{R}_3|$. This suggests that one may integrate not along the real axis itself but along a contour in the first quadrant of the complex plane that begins at large r where an asymptotic solution is valid, and ends on the real axis.[6] For concreteness, we note that the ratio of solutions obtained from Eq. (61) should, for large $r_\star$, be

$$\left|\frac{\mathcal{R}_3}{\mathcal{R}_4}\right|^{1/2} \propto |r_\star^2 \mathrm{e}^{\mathrm{i}\omega r_\star}| \propto [(\Re r_\star)^2 + (\Im r_\star)^2]\exp(-\omega \Im r_\star). \quad (62)$$

To evaluate $\mathcal{R}_3$ at some real r_0, we integrate along the path

$$\Im r = \min\left\{\frac{3}{\omega}\ln\frac{\Re r}{r_0}, \Re r\right\}, \quad (63)$$

for which $\mathcal{R}_4$ dominates as $\Re r \to \infty$. In practice, we follow such a path directly to $r_0 = r$ if we desire $\mathcal{R}_3(r)$ at $r > r_{\mathrm{f}} \equiv \max\{|\omega|^{-1}, 3M\}$; for $r < r_{\mathrm{f}}$, we integrate first to r_{f} and then leftward along the real axis. We have experimented with both the RK4 integrator and a Bulirsch-Stoer method[7]; we have used the Bulirsch-Stoer integrator here since it is slightly faster for similar accuracy, but we found both methods to be workable.

The starting point for the integration is initialized in accordance with Press & Teukolsky (1973, Eq. D15) using terms through order r^{-2} (i.e. C_2); our default starting value of $\Re r$ is $1250\max\{M, |\omega|^{-1}\}$.

4.3 Source term

We next need the source term $\mathcal{T}_{\ell m\omega}(r)$ in the Teukolsky equation. This is given by[8] as

$$\mathcal{T}_{\ell m\omega}(r) = \int \mathrm{d}t\, \mathcal{T}_{\ell,m}(r,t)\,\mathrm{e}^{\mathrm{i}\omega t}, \quad (64)$$

where

$$\mathcal{T}_{\ell,m}(r,t) = \Delta^2(r)\{A_0\delta(r-r_0) + \partial_r[A_1\delta(r-r_0)] \\ + \partial_r^2[A_2\delta(r-r_0)]\}. \quad (65)$$

Here r_0 denotes the radial coordinate of the particle at time t, and the A-coefficients are given as follows: for the δ-function,

$$A_0 = -2\frac{\Sigma}{\rho^2\Delta^2}[\mathbb{L}_1^\dagger \mathbb{L}_2^\dagger S + 2\mathrm{i}a\rho\sin\theta\,\mathbb{L}_2^\dagger S]C_{nn} \\ + \frac{2\sqrt{2}}{\rho^3\Delta}\Big[\Big(\frac{\mathrm{i}K}{\Delta} + \frac{2r}{\Sigma}\Big)\mathbb{L}_2^\dagger S \\ - \Big(\frac{\mathrm{i}K}{\Delta} - \frac{2r}{\Sigma}\Big)\frac{2a^2\sin\theta\cos\theta}{\Sigma}S\Big]C_{n\bar{m}} \\ + \frac{\bar{\rho}}{\rho^3}\Big[\frac{K^2}{\Delta^2} + 2\mathrm{i}\rho\frac{K}{\Delta} + \mathrm{i}\frac{2\Delta\omega r - 2K(r-M)}{\Delta^2}\Big]SC_{\bar{m}\bar{m}}; \quad (66)$$

for the derivative of the δ-function[9],

$$A_1 = -\frac{2\sqrt{2}}{\rho^3\Delta}\Big[\mathbb{L}_2^\dagger S + \frac{2a^2\sin\theta\cos\theta}{\Sigma}S\Big]C_{n\bar{m}} \\ + \frac{2\bar{\rho}}{\rho^3}\Big(\rho - \mathrm{i}\frac{K}{\Delta}\Big)SC_{\bar{m}\bar{m}}, \quad (67)$$

and for the second derivative of the δ-function,

$$A_2 = -\frac{\bar{\rho}}{\rho^3}SC_{\bar{m}\bar{m}}, \quad (68)$$

where we have suppressed the arguments of the spheroidal harmonic $S \equiv S_{\ell,m}^{-2,a\omega}(\theta,\phi)$. The coefficients of the stress-energy tensor are

$$C_{ab} = \mu\frac{(\boldsymbol{u}\cdot\boldsymbol{a})(\boldsymbol{u}\cdot\boldsymbol{b})}{\Sigma u^t}, \quad (69)$$

where $\boldsymbol{a}$ and $\boldsymbol{b}$ are null vectors (either $\boldsymbol{n}$ or $\bar{\boldsymbol{m}}$). The values of $\mathbb{L}_1^\dagger\mathbb{L}_2^\dagger S$ and $\mathbb{L}_2^\dagger S$ can be obtained from Eqs. (A8) and (A10).

Now for a quasiperiodic trajectory along the torus, we may write $\mathcal{T}_{\ell,m}(r,t)$ as a function of the angle variables, $\mathcal{T}_{\ell,m}(r,t) = \mathcal{T}_{\ell,m}[r,\boldsymbol{\psi}(t)]$, where each $\psi_i(t)$ advances at the rate $\dot{\psi}_i = \Omega_i$. Then we take the Fourier transform,

$$\mathcal{T}_{\ell,m}(r,\boldsymbol{\psi}) = \sum_{\boldsymbol{q}}\mathcal{T}_{\ell,m}(r|\boldsymbol{q})\mathrm{e}^{-\mathrm{i}\boldsymbol{q}\cdot\boldsymbol{\psi}}, \quad (70)$$

where $\boldsymbol{q}$ is a lattice vector (i.e. q_r, q_θ, and q_ϕ are all integers). Using $\boldsymbol{\psi} = \boldsymbol{\psi}^{(0)} + \boldsymbol{\Omega}t$, we may integrate Eq. (64) to get:

$$\mathcal{T}_{\ell m\omega}(r) = \sum_{\boldsymbol{q}}\mathcal{T}_{\ell,m}(r|\boldsymbol{q})\mathrm{e}^{\mathrm{i}\boldsymbol{q}\cdot\boldsymbol{\psi}^{(0)}}2\pi\delta(\omega - \boldsymbol{\Omega}\cdot\boldsymbol{q}). \quad (71)$$

With Eq. (71), we may evolve each value of $\boldsymbol{q}$ separately, treating $\mathcal{T}_{\ell,m}(r|\boldsymbol{q})$ as the source, and then sum the resulting perturbations.

The Fourier components $\mathcal{T}_{\ell,m}(r|\boldsymbol{q})$ may be evaluated as follows. We first see that

$$\mathcal{T}_{\ell,m}(r|\boldsymbol{q}) = \int\frac{\mathrm{d}^3\boldsymbol{\psi}}{(2\pi)^3}\mathcal{T}_{\ell,m}(r,\boldsymbol{\psi})\mathrm{e}^{\mathrm{i}\boldsymbol{q}\cdot\boldsymbol{\psi}}. \quad (72)$$

Now if we increment ψ^ϕ by some amount $\delta\psi^\phi$, then it is easy to see that ϕ is increased by $\delta\psi^\phi$ while the other phase space coordinates $\{r,\theta,u_r,u_\theta,u_\phi\}$ remain fixed. Thus $\mathcal{T}_{\ell,m}(r,\boldsymbol{\psi})$ is multiplied by $\exp(-\mathrm{i}m\delta\psi^\phi)$. Since the complex exponential in Eq. (72) is multiplied by $\exp(\mathrm{i}q_\phi\delta\psi_\phi)$, it follows that

$\mathcal{T}_{\ell,m}(r|\boldsymbol{q})$ is nonzero only if $q_\phi = m$. In this case, the ψ^ϕ integral is also trivial, so we find

$$\mathcal{T}_{\ell,m}(r|\boldsymbol{q}) = \delta_{m,q_\phi} \int \frac{\mathrm{d}\psi^r \, \mathrm{d}\psi^\theta}{(2\pi)^2} \, \mathcal{T}_{\ell,m}(r,\boldsymbol{\psi})\mathrm{e}^{\mathrm{i}\boldsymbol{q}\cdot\boldsymbol{\psi}}. \quad (73)$$

This provides a means of computing $\mathcal{T}_{\ell,m}(r|\boldsymbol{q})$ while doing only a double integral over the torus instead of a triple integral. In practical computation, the integral is computed as a discretized sum over $N_r N_\theta$ equally spaced points on the $\psi^\phi = 0$ subtorus. This completes the approximation of $\mathcal{T}_{\ell,m}(r|\boldsymbol{q})$ by a finite sum over δ-functions and their derivatives.

4.4 Solution to the inhomogeneous radial Teukolsky equation

We solve the full radial Teukolsky equation via a Green's function method. The starting point is to recognize that given the boundary conditions, the solution must satisfy

$$\mathcal{R}(r) = \begin{cases} Z^{\mathrm{down}}\mathcal{R}_1(r) & r < r_1 \\ Z^{\mathrm{out}}\mathcal{R}_3(r) & r > r_1 \end{cases}, \quad (74)$$

where $Z^{\mathrm{down, \ out}}$ are undetermined constants. We now suppose that the source contained a δ-function at some radius r_1, i.e. we had an inhomogeneous equation,

$$\Delta^2 \frac{\mathrm{d}}{\mathrm{d}r}\left(\Delta^{-1}\frac{\mathrm{d}\mathcal{R}}{\mathrm{d}r}\right) - V\mathcal{R} = -\delta(r - r_1). \quad (75)$$

This would imply the jump conditions that R be continuous at r_1 and that its derivative jump by

$$\mathcal{R}'(r_1 + \epsilon) - \mathcal{R}'(r_1 - \epsilon) = \frac{1}{\Delta(r_1)}. \quad (76)$$

These two conditions allow us to solve for $Z^{\mathrm{down, \ out}}$:

$$Z^{\mathrm{down}} = \frac{\mathcal{R}_3(r_1)}{\Delta(r_1)W_{31}(r_1)} \quad \text{and} \quad Z^{\mathrm{out}} = \frac{\mathcal{R}_1(r_1)}{\Delta(r_1)W_{31}(r_1)}, \quad (77)$$

where the Wronskian is

$$W_{31}(r) = \mathcal{R}_3(r)\mathcal{R}_1'(r) - \mathcal{R}_1(r)\mathcal{R}_3'(r). \quad (78)$$

The Wronskian of the two solutions to a second-order ODE may be obtained by elementary means: in this case, we have $W(r) \propto \Delta(r)$, so we write $W_{31}(r) = \aleph\Delta(r)$. An evaluation at one point is sufficient to determine $\aleph$.

We thus have the full solution in the interior region $(r < r_-)$

$$\mathcal{R}_{\ell m\omega}(r) = \sum_{\boldsymbol{q}} Z_{\ell m,\boldsymbol{q}}^{\mathrm{down}}\mathcal{R}_1(r)\mathrm{e}^{\mathrm{i}\boldsymbol{q}\cdot\boldsymbol{\psi}^{(0)}} \, 2\pi\delta(\omega - \boldsymbol{q}\cdot\boldsymbol{\Omega}), \quad (79)$$

where integration of the Green's function gives

$$Z_{\ell m,\boldsymbol{q}}^{\mathrm{down}} = \aleph_{\ell m\omega}^{-1}\int [A_0\mathcal{R}_3 - A_1\mathcal{R}_3' + A_2\mathcal{R}_3'']\, \mathrm{e}^{\mathrm{i}\boldsymbol{q}\cdot\boldsymbol{\psi}}\, \frac{\mathrm{d}^3\boldsymbol{\psi}}{(2\pi)^3}, \quad (80)$$

and A_0 and $\mathcal{R}_3$ are evaluated at the particle position. (The A_1 and A_2 terms are obtained similarly using integration by parts to move the radial derivative from the argument of $\mathcal{T}$ to the argument of the Green's function.) A similar equation is valid in the exterior region $r > r_+$ for the outgoing wave amplitude $Z_{\ell m,\boldsymbol{q}}^{\mathrm{out}}$ if we swap $\mathcal{R}_1 \leftrightarrow \mathcal{R}_3$.

Using Eq. (43), it follows that in the interior region,

$$\psi_4 = \rho^4 \sum_{\ell m,\boldsymbol{q}} Z_{\ell m,\boldsymbol{q}}^{\mathrm{down}}\mathcal{R}_1(r)S_{\ell,m}^{-2,a\omega}(\theta)\mathrm{e}^{\mathrm{i}m\phi}\mathrm{e}^{\mathrm{i}\boldsymbol{q}\cdot\boldsymbol{\psi}^{(0)}}\mathrm{e}^{-\mathrm{i}\omega t}, \quad (81)$$

and in the exterior region

$$\psi_4 = \rho^4 \sum_{\ell m,\boldsymbol{q}} Z_{\ell m,\boldsymbol{q}}^{\mathrm{out}}\mathcal{R}_3(r)S_{\ell,m}^{-2,a\omega}(\theta)\mathrm{e}^{\mathrm{i}m\phi}\mathrm{e}^{\mathrm{i}\boldsymbol{q}\cdot\boldsymbol{\psi}^{(0)}}\mathrm{e}^{-\mathrm{i}\omega t}. \quad (82)$$

At large radii, $\rho^4\mathcal{R}_3 \to r^{-1}\mathrm{e}^{\mathrm{i}\omega r_\star}$. Then, since the flux of gravitational waves at large radii is the time-average of $|\psi_4|^2/(4\pi\omega^2)$, we may integrate over the sphere (using $\int |S|^2 \sin\theta \, \mathrm{d}\theta \, \mathrm{d}\phi = 2\pi$) to get the emitted power to ∞:

$$P_{\mathrm{out}} = \sum_{\ell,m,\boldsymbol{q}} \frac{|Z_{\ell m,\boldsymbol{q}}^{\mathrm{out}}|^2}{2\omega^2}, \quad (83)$$

where $\omega = \boldsymbol{q}\cdot\boldsymbol{\Omega}$. The power emitted into the black hole was derived by Teukolsky & Press (1974); the solution is

$$P_{\mathrm{down}} = \sum_{\ell,m,\boldsymbol{q}} \alpha\frac{|Z_{\ell m,\boldsymbol{q}}^{\mathrm{down}}|^2}{2\omega^2}, \quad (84)$$

where

$$\alpha = \frac{8192M^5 r_{\mathrm{h}+}^5\varpi(\varpi^2 + \Gamma^2)(\varpi^2 + 4\Gamma^2)\omega^3}{|C|^2}. \quad (85)$$

Here C is the Starobinsky-Teukolsky coefficient, whose squared absolute value is

$$\begin{aligned} |C|^2 = & \ [(\lambda + 2)^2 + 4m\chi - 4\chi^2](\lambda^2 + 36m\chi - 36\chi^2) \\ & + 48(2\lambda + 3)\chi(2\chi - m) + 144\omega^2(M^2 - a^2), \end{aligned} \quad (86)$$

and we have used $\chi = a\omega$ and $\varpi = \omega - m\Omega_{\mathrm{H}}$.[10]

The energy and angular momentum radiated (both to infinity and into the hole) are required in order to follow the evolution of circular *or* equatorial orbits under radiation reaction (e.g. Detweiler 1978; Shibata 1993, 1994; Kennefick 1998; Hughes 2000); comparison of $\dot{\mathcal{E}}$ and $\dot{\mathcal{L}}$ to literature values can be used a test of our code. Evolution of generic orbits that are both eccentric and inclined would also require a relation for $\dot{\mathcal{Q}}$ (Mino 2003; Hughes et al. 2005; Drasco & Hughes 2006), which is not required for this paper.

We have tested our code by checking our computed energy and angular momentum fluxes against the results from Table VI of Drasco & Hughes (2006), for $M = 1$, $a_\star = 0.9$, semilatus rectum $p \equiv 2/(r_-^{-1} + r_+^{-1}) = 6$, and a range of eccentricities e [defined by $r_+/r_- = (1 + e)/(1 - e)$] and inclinations $\theta_{\mathrm{inc}} \equiv \pi/2 - \theta_{\mathrm{min}}$. We consider all modes with $\max\{\ell, |q_\phi|, |q_\theta|, |q_r|\} \leqslant j_{\mathrm{max}}$, and expect convergence as $n \to \infty$. Comparisons are given in Table 1.

5 THE RESONANT AMPLITUDE

Having now solved for ψ_4, it remains to compute the resonant amplitude $\mathcal{S}^{(m)}$ from Paper I. While it would in principle be possible to compute the metric perturbation directly, by constructing the master potential Ψ (Wald 1978; Ori 2003) and then utilizing the Chrzanowski (1975) procedure, we will find it more useful to express $\mathcal{S}^{(m)}$ directly in terms of ψ_4.

---

[10] Note that Hughes (2000, Eq. 4.18) contains a missing factor of m in the first term; $[(\lambda + 2)^2 + 4a\omega_{mk} - 4a^2\omega_{mk}^2]$ should read $[(\lambda + 2)^2 + 4ma\omega_{mk} - 4a^2\omega_{mk}^2]$. Also note that "$\epsilon$" as defined in Teukolsky & Press (1974) is $\Gamma/2$ here.

Table 1. Comparison of our energy and angular momentum fluxes at ∞ and at the horizon to those of Drasco & Hughes (2006) (DH) for $M = 1$, $a_\star = 0.9$, and semilatus rectum 6. The "Error" column gives the maximum fractional error of any of the four columns relative to DH.

e	$\theta_{\rm inc}$	$j_{\rm max}$	$\dot{E}^{\rm H}/\mu^2$	$\dot{E}^\infty/\mu^2$	$\dot{L}^{\rm H}/\mu^2$	$\dot{L}^\infty/\mu^2$	Error
0.1	20°	4	−4.2574E−6	+5.8126E−4	−6.7238E−5	+8.4497E−3	1.1E−2
		6	−4.2576E−6	+5.8700E−4	−6.7241E−5	+8.5310E−3	6.8E−4
		8	−4.2576E−6	+5.8738E−4	−6.7241E−5	+8.5362E−3	3.6E−5
		DH	−4.2576E−6	+5.8740E−4	−6.7241E−5	+8.5365E−3	
0.3	40°	4	−5.8169E−6	+7.0118E−4	−1.0006E−4	+7.6189E−3	3.7E−2
		6	−5.8857E−6	+7.2361E−4	−1.0061E−4	+7.8091E−3	4.4E−3
		8	−5.8882E−6	+7.2636E−4	−1.0063E−4	+7.8316E−3	5.8E−4
		DH	−5.8882E−6	+7.2678E−4	−1.0063E−4	+7.8350E−3	

Furthermore, since we are considering Lindblad resonances, the metric perturbations are required only in the interior and exterior regions, i.e. at radii $r < r_-$ or $r > r_+$, where the vacuum Einstein equation is obeyed. This will simplify our task greatly.

The key to the computation of the resonant amplitude is the result from Paper I that

$$\mathcal{S}^{(m)} = \frac{2\mathrm{i}}{m\Omega_{\rm s}\mu_1 \mathcal{Z}\epsilon}\mathcal{P}^{(m)}, \qquad (87)$$

where $\mathcal{P}^{(m)}$ is the power provided by the m Fourier mode of the metric perturbation to a test particle of mass $\mu_1 \to 0$ on an orbit that is slightly eccentric, oscillating between $R - \epsilon$ and $R + \epsilon$, where ϵ is small.

The power can be computed without direct knowledge of the metric perturbations, but it breaks into two similar cases for the ILRs and OLRs. In both cases, we use the fact that knowledge of ψ_4 in a neighborhood around the test particle's radius enables determination of the metric perturbations (up to gauge modes and to the zero-frequency "$\ell = 0$ and 1 modes" corresponding to changes in the mass and spin of the hole, which provide no power) and hence the power is the same as that which would be provided by a pure gravitational wave solution with the same ψ_4.

The perturber in our case is on a circular equatorial orbit, hence $\tilde{J}_r = \tilde{J}_\theta = 0$ and no $q_r, q_\theta \neq 0$ need be considered. The mode of interest has $q_\phi = m$, $\omega = m\Omega_{\rm s}$, and pattern speed $\Omega_{\rm s} = \Omega_\phi$ (evaluated at the perturber position). Without loss of generality, we set the initial longitude $\psi_\phi^{(0)} = 0$.

5.1 Inner Lindblad resonances

In the case of an ILR, the Weyl tensor component ψ_4 is given by Eq. (81). This is exactly the same as the case of an incoming gravitational wave with azimuthal quantum number m and frequency $\omega = m\Omega_{\rm s}$ with the specified amplitudes in each ℓ mode. In such a situation, one may see that the radial mode is

$$\mathcal{R}_{\ell m\omega}(r) = Z_{\ell m}^{\rm down}\mathcal{R}_1(r) = Z_{\ell m}^{\rm down}[c_{13}\mathcal{R}_3(r) + c_{14}\mathcal{R}_4(r)], \qquad (88)$$

where c_{13} and c_{14} are constants evaluated in Appendix B. The power in incoming gravitational waves, outgoing waves,

and waves going down into the hole are given by

$$P_{\rm in} = \frac{(2\omega)^8}{|C|^2}\frac{|c_{14}Z_{\ell m}^{\rm down}|^2}{2\omega^2},$$

$$P_{\rm out} = \frac{|c_{13}Z_{\ell m}^{\rm down}|^2}{2\omega^2}, \text{ and}$$

$$P_{\rm down} = \frac{\alpha|Z_{\ell m}^{\rm down}|^2}{2\omega^2}. \qquad (89)$$

Now we consider our test particle. It too emits gravitational waves, including a set of modes at azimuthal quantum number m and at the frequency

$$\omega = m\Omega(R) - \kappa = m\Omega_{\rm s}. \qquad (90)$$

These waves are emitted both down into the hole and out to infinity, with amplitudes $Z_{1,\ell m}^{\rm down}$ and $Z_{1,\ell m}^{\rm out}$ that are calculable by the same procedure as for the perturber, but this time with Fourier modes $(q_r, q_\theta, q_\phi) = (-1, 0, m)$.

We may now obtain the power absorbed by the test particle using conservation of energy. There is a correction to the power escaping to ∞ and down the black hole in accordance with

$$\delta P_{\rm out} = \Re\sum_{\ell m}\frac{c_{13}Z_{\ell m}^{\rm down}Z_{1,\ell m}^{\rm out*}}{\omega^2} \text{ and}$$

$$\delta P_{\rm down} = \Re\sum_{\ell m}\frac{\alpha Z_{\ell m}^{\rm down}Z_{1,\ell m}^{\rm down*}}{\omega^2}. \qquad (91)$$

The power absorbed by the test particle is the negative of this, which can be found by expanding the real part as one-half the sum of a quantity and its complex conjugate:

$$\sum_{m\in\mathbb{Z}}\mathcal{P}^{(m)} = -\delta P_{\rm out} - \delta P_{\rm down}$$

$$= -\frac{1}{2\omega^2}\sum_{\ell m}Z_{\ell m}^{\rm down}\left(c_{13}Z_{1,\ell m}^{\rm out*} + \alpha Z_{1,\ell m}^{\rm down*}\right)$$

$$\qquad -\frac{1}{2\omega^2}\sum_{\ell m}Z_{\ell m}^{\rm down*}\left(c_{13}^*Z_{1,\ell m}^{\rm out} + \alpha Z_{1,\ell m}^{\rm down}\right). \quad (92)$$

We may identify the individual contributions $\mathcal{P}^{(m)}$ by noting that it is linear in the m Fourier mode of the metric perturbation; and thus it arises from the terms proportional

to $Z_{\ell m}^{\text{down}}$ or $Z_{\ell,-m}^{\text{down}*}$.[11] Therefore:

$$\mathcal{P}^{(m)} = -\frac{1}{2\omega^2} \sum_{\ell} Z_{\ell m}^{\text{down}} \left(c_{13} Z_{1,\ell m}^{\text{out}*} + \alpha Z_{1,\ell m}^{\text{down}*} \right)$$
$$- \frac{1}{2\omega^2} \sum_{\ell} Z_{\ell,-m}^{\text{down}*} \left(c_{13-}^* Z_{1,\ell,-m}^{\text{out}} + \alpha_- Z_{1,\ell,-m}^{\text{down}} \right). \quad (93)$$

Here c_{13-} refers to the coefficient for negative values of m and ω: $c_{13-}(\ell, m, \omega) \equiv c_{13}(\ell, -m, -\omega)$, and similarly for α_- (note that the α-coefficients are real). Inspection of the radial equation shows that $c_{13-}^* = c_{13}$ and $\alpha_- = \alpha$. In the particular case where both the perturber and the test particle are in the equatorial plane, there also exists a reflection symmetry of the emitted waveform across the equator, e.g. $Z_{\ell,-m}^{\text{down}*} = (-1)^m Z_{\ell m}^{\text{down}}$. Therefore the two terms in Eq. (93) are equal. Thus we see that the power absorbed by the test particle in all of the frequency ω modes is

$$\mathcal{P}^{(m)} = -\frac{1}{\omega^2} \sum_{\ell} Z_{\ell m}^{\text{down}} \left(c_{13} Z_{1,\ell m}^{\text{out}*} + \alpha Z_{1,\ell m}^{\text{down}*} \right). \quad (94)$$

This has the correct dependences: it is manifestly linear in μ_1, which is essential since the computation of the resonant amplitude requires division by μ_1, and also it is linear in the epicyclic oscillation amplitude ϵ since the order q_r Fourier mode of the gravitational wave scales as $\epsilon^{|q_r|}$.

5.2 Outer Lindblad resonances

A related argument applies to the OLRs. This time, we consider a perturber on a circular orbit, again emitting at frequency $\omega = m\Omega_{\text{s}}$, and a test particle on a slightly eccentric orbit emitting at frequency

$$\omega = m\Omega(R) + \kappa, \quad (95)$$

i.e. we are considering the $(q_r, q_\theta, q_\phi) = (1, 0, m)$ Fourier mode on its torus. This time, since we are considering a vacuum solution outside the perturber's orbit, the perturber (or at least its $m \neq 0$ part) may be replaced by a gravitational wave coming out of the hole's past horizon. The radial mode amplitude is now

$$\mathcal{R}_{\ell m \omega}(r) = Z_{\ell m}^{\text{out}} \mathcal{R}_3(r) = Z_{\ell m}^{\text{down}} [c_{31} \mathcal{R}_1(r) + c_{32} \mathcal{R}_2(r)]. \quad (96)$$

The changes in power escaping to infinity and going down into the hole are now

$$\delta P_{\text{out}} = \Re \sum_{\ell m} \frac{Z_{\ell m}^{\text{out}} Z_{1,\ell m}^{\text{out}*}}{\omega^2} \quad \text{and}$$
$$\delta P_{\text{down}} = \Re \sum_{\ell m} \frac{\alpha c_{31} Z_{\ell m}^{\text{out}} Z_{1,\ell m}^{\text{down}*}}{\omega^2}; \quad (97)$$

but we note that Eq. (B14) implies $\alpha c_{31} = -c_{13}^*$. The power absorbed by the test particle from the m Fourier mode of the metric perturbation is now

$$\mathcal{P}^{(m)} = -\frac{1}{\omega^2} \sum_{\ell} Z_{\ell m}^{\text{out}} \left(Z_{1,\ell m}^{\text{out}*} - c_{13}^* Z_{1,\ell m}^{\text{down}*} \right). \quad (98)$$

---

[11] Since ψ_4 is a complex quantity whose real and imaginary parts encode different components of the Weyl tensor, perturbations in the metric tensor, curvature, etc. are not linear in ψ_4 alone but rather are linear in ψ_4 and ψ_4^*. Thus the m Fourier mode of the metric perturbation depends on both the m and $-m$ Fourier modes of ψ_4.

Equations (94) and (98) at first appear remarkable: they show that the torques at the Lindblad resonances, which depend on $\mathcal{S}^{(m)}$, can be related to the overlap between the gravitational waveforms emitted by the perturber and a test particle at the location of the resonance. But this could have been expected: the same time-dependent multipole moments that are responsible for the gravitational wave emission also generate resonant torques.

We are now ready to compute the resonant amplitudes $\mathcal{S}^{(m)}$. We consider three cases. First we review the case of a Keplerian disc, showing how the Lindblad torques can be treated via the Teukolsky formalism. Then we consider a disc around a Schwarzschild black hole with a perturber, similar to the physical situation envisaged by Chang et al. (2010); this is the first case for which the relativistic machinery developed in Paper I and here is actually necessary, and we find an additional $m = 1$ ILR with no Keplerian analogue.[12] Finally, we compute the resonance strengths in the case of an equatorial orbit around a Kerr black hole.

6 RESONANCES IN THE KEPLER PROBLEM

The problem of Lindblad resonance torques in Keplerian discs has been treated many times; here we treat it using the Teukolsky equations. We wish to find $|\mathcal{S}^{(m)}|^2$ for each resonance. This requires us first to find $Z_{\ell m,\boldsymbol{q}}^{\text{out,down}}$ for both circular orbits (the perturber) and slightly eccentric orbits (for the test particle). We work at radii $\gg M$. The solutions for the radial Teukolsky functions in this regime are described in Appendix C; the angular functions are simply the spin-weighted spherical harmonics. As is well-known, the Lindblad resonances can be found at values of the test particle radius

$$r_1 = \left(\frac{m \mp 1}{m} \right)^{2/3} r_0 \equiv \varsigma_m^\mp r_0, \quad (99)$$

where the upper and lower signs refer to the inner and outer Lindblad resonances.

6.1 Emitted waves: circular orbit

We consider first a particle on a circular Keplerian orbit at radius $r_0 \gg M$, orbiting at angular velocity $\Omega_\phi = M^{1/2} r_0^{-3/2}$. The required stress-energy coefficients phased to zero longitude are

$$C_{nn} = \frac{\mu}{4r_0^2}, \quad C_{n\bar{m}} = \frac{-\mathrm{i}\mu M^{1/2}}{2\sqrt{2}\, r_0^{5/2}}, \quad \text{and} \quad C_{\bar{m}\bar{m}} = -\frac{\mu M}{2r_0^3}. \quad (100)$$

The leading-order source term is then

$$A_0 = -\frac{\mu}{2r_0^2} \mathbb{L}_1^\dagger \mathbb{L}_2^\dagger S\left(\theta = \frac{\pi}{2} \right). \quad (101)$$

(the A_1 and A_2 terms have powers of $r_0^{-3/2}$ and r_0^{-1} respectively; when they are integrated, the additional ∂_r or ∂_r^2

---

[12] The new ILR does however exist for any Newtonian potential with an ISCO.

makes these subdominant to A_0). We will find it convenient to define

$$
\begin{aligned}
y_{\ell m} &\equiv \mathbb{L}_1^\dagger \mathbb{L}_2^\dagger S\left(\theta = \frac{\pi}{2}\right) \\
&= \sqrt{2\pi \frac{(\ell+2)!}{(\ell-2)!}}\, Y_{\ell m}\left(\theta = \frac{\pi}{2}, \phi = 0\right)
\end{aligned}
\tag{102}
$$

so that $A_0 = -\mu y_{\ell m}/(2r_0^2)$.

Now for the circular orbit, a particular m-mode is excited only at $\omega = m\Omega_\phi = mM^{1/2}r_0^{-3/2}$, and the Fourier mode of the torus that excites it is $(q_r, q_\theta, q_\phi) = (0, 0, m)$. The downward and outward radiation amplitudes are obtained from Eq. (80), with the formulae for $\mathcal{R}_1$, $\mathcal{R}_3$, and $\aleph$ from Appendix C:

$$
\begin{aligned}
Z_{\ell m;0,0,m}^{\mathrm{down}} &= \frac{\mathcal{R}_3(r_0)A_0}{\aleph} = \frac{\mu y_{\ell m}}{2(2\ell+1)k_1 r_0^{\ell+1}} \quad \text{and} \\
Z_{\ell m;0,0,m}^{\mathrm{out}} &= \frac{\mathcal{R}_1(r_0)A_0}{\aleph} = \mathrm{i}^{2-\ell}\frac{(\ell-2)!\,\mu y_{\ell m}(2\omega)^{\ell+2}r_0^\ell}{2\cdot(2\ell+1)!}.
\end{aligned}
\tag{103}
$$

Note the $\propto r_0^{-(\ell+1)}$ and $\propto r_0^\ell$ radial behaviour; this is expected for sourcing the order-ℓ multipole.

6.2 Emitted waves: eccentric orbit

We now consider a test particle of mass μ_1 orbiting at radius r_1, and with slight eccentricity ϵ/r_1 such that the particle oscillates between $r_1 - \epsilon$ and $r_1 + \epsilon$. We are now interested in the $(\mp 1, 0, m)$ Fourier mode (where as in Paper I the upper sign represents the ILR and the lower sign the OLR), which has frequency $\omega = (m \mp 1)M^{1/2}r_1^{-3/2}$. As this is a resonance we will not distinguish between this value of ω and that for the perturber.

The computation of A_0 and negligibility of $A_{1,2}$ proceed in an exactly analogous way to that for the circular orbit; the only differences are that (i) the true radius r differs from its mean value r_1; and (ii) we must now work at general longitude since we no longer have trivial angle integrals, introducing a phase factor:

$$
A_0 = -\frac{\mu_1 y_{\ell m}}{2r^2}\mathrm{e}^{-\mathrm{i}m\phi}.
\tag{104}
$$

This time the integral over the radial angle ψ^r is nontrivial: we find

$$
Z_{1;\ell m;\mp 1,0,m}^{\mathrm{down}} = \int_0^{2\pi} \frac{\mathcal{R}_3(r)A_0}{\aleph}\mathrm{e}^{\mp \mathrm{i}\psi^r}\frac{\mathrm{d}\psi_r}{2\pi}
\tag{105}
$$

(where the integrand may be evaluated at $\psi^\phi = 0$ since the ψ^ϕ integral is trivial), and $Z_{\ell m;\mp 1,0,m}^{\mathrm{out}}$ may be obtained by replacing with $\mathcal{R}_1(r)$.

The epicyclic motion in the Kepler potential can be found in any dynamics text (e.g. Murray & Dermott 2000); expressed in our variables, it is, at $\psi^\phi = 0$,

$$
r = r_1 - \epsilon\cos\psi^r, \quad \text{and} \quad \phi = 2\frac{\epsilon}{r_1}\sin\psi^r.
\tag{106}
$$

To first order in ϵ, we then have

$$
\int_0^{2\pi} r^n \mathrm{e}^{-\mathrm{i}m\phi}\mathrm{e}^{\mp \mathrm{i}\psi^r}\frac{\mathrm{d}\psi^r}{2\pi} = \left(-\frac{n}{2} \mp m\right)\epsilon r_1^{n-1}.
\tag{107}
$$

Therefore, we conclude that

$$
\begin{aligned}
Z_{1;\ell m;\mp 1,0,m}^{\mathrm{down}} &= \frac{\mu_1 \epsilon y_{\ell m}}{2(2\ell+1)k_1 r_1^{\ell+2}}\left(\frac{\ell+1}{2} \mp m\right) \quad \text{and} \\
Z_{1;\ell m;\mp 1,0,m}^{\mathrm{out}} &= \mathrm{i}^{2-\ell}\frac{(\ell-2)!\,\mu_1 \epsilon y_{\ell m}(2\omega)^{\ell+2}r_1^{\ell-1}}{2\cdot(2\ell+1)!} \\
&\quad \times \left(-\frac{\ell}{2} \mp m\right).
\end{aligned}
\tag{108}
$$

6.3 Resonant amplitudes

We are now ready to evaluate Eqs. (94) and (98), each of which has two terms. We focus on the ILRs; the treatment of the OLRs is analogous. A comparison of the two terms shows that, using Eq. (108) and the relations in Appendix C,

$$
\left|\frac{\alpha Z_{1;\ell m;\mp 1,0,m}^{\mathrm{down}}}{c_{13} Z_{1;\ell m;\mp 1,0,m}^{\mathrm{out}}}\right| \sim |\varpi|M\left(\frac{M}{r_1}\right)^{2\ell+1} \ll 1,
\tag{109}
$$

so the $Z_{1;\ell m;\mp 1,0,m}^{\mathrm{out}}$ term dominates in Eq. (94). The actual evaluation using Eq. (103) as well gives

$$
\mathcal{P}^{(m)} = -\mathrm{i}\mu\mu_1\epsilon\omega\sum_{\ell=m}^{\infty}\frac{(\ell-2)!}{(\ell+2)!}\frac{(\ell+2m)y_{\ell m}^2}{2\ell+1}\frac{r_1^{\ell-1}}{r_0^{\ell+1}}.
\tag{110}
$$

The summation in Eq. (110) can be simplified using:

$$
\begin{aligned}
\frac{(\ell-2)!y_{\ell m}^2}{(\ell+2)!(2\ell+1)} &= \frac{1}{4\pi}\int_0^{2\pi}P_\ell(\cos\phi)\cos(m\phi)\,\mathrm{d}\phi \\
&= \frac{1}{4\pi(\ell!)}\frac{\mathrm{d}^\ell}{\mathrm{d}\varsigma^\ell}\int_0^{2\pi}\left.\frac{\cos(m\phi)\,\mathrm{d}\phi}{\sqrt{1+\varsigma^2-2\varsigma\cos\phi}}\right|_{\varsigma=0} \\
&= \frac{1}{4(\ell!)}\frac{\mathrm{d}^\ell}{\mathrm{d}\varsigma^\ell}\left.b_{1/2}^{(m)}(\varsigma)\right|_{\varsigma=0}.
\end{aligned}
\tag{111}
$$

Here the first equality arises by considering the spherical harmonic addition theorem, applying it to points on the equator at longitudes 0 and ϕ, and taking the Fourier transform over ϕ; the second from the generating function relation for the Legendre polynomials; and the third from the definition of the Laplace coefficient. With this, and using the Taylor expansion formula (and the fact that the Taylor series of $b_{1/2}^{(m)}$ begins with the order ς^m term for $m \geqslant 0$), we find

$$
\mathcal{P}^{(m)} = -\mathrm{i}\frac{\mu\mu_1\epsilon\omega}{4r_0^2}\left[b_{1/2}^{(m)\prime}(\varsigma_m^-) + \frac{2mb_{1/2}^{(m)}(\varsigma_m^-)}{\varsigma_m^-}\right],
\tag{112}
$$

where here the $'$ on the Laplace coefficient denotes differentiation with respect to the argument. It follows that

$$
\mathcal{S}^{(m)} = \frac{\mu\omega}{2m\Omega_{\mathrm{s}}\mathcal{Z}\varsigma_m^- r_0^2}[\varsigma_m^- b_{1/2}^{(m)\prime}(\varsigma_m^-) + 2mb_{1/2}^{(m)}(\upsilon_m^-)].
\tag{113}
$$

The prefactor simplifies using $\Omega_{\mathrm{s}} = M^{1/2}/r_0^{3/2}$ and $\omega = m\Omega_{\mathrm{s}}$, leaving us with

$$
\mathcal{S}^{(m)} = \frac{qM^{1/2}(\varsigma_m^-)^{1/2}}{2r_0^{1/2}}[\varsigma_m^- b_{1/2}^{(m)\prime}(\varsigma_m^-) + 2mb_{1/2}^{(m)}(\varsigma_m^-)].
\tag{114}
$$

This is equivalent to the result from Paper I using the Newtonian potential h_{tt}.

For the OLRs, a similar argument holds: the $c_{13}^* Z_{1,\ell m}^{\mathrm{down}*}$

term dominates over $Z_{1,\ell m}^{\text{out}}$ in Eq. (98), yielding

$$\mathcal{P}^{(m)} = -\mathrm{i}\mu\mu_1\epsilon\omega \sum_{\ell=\max\{m,2\}}^{\infty} \frac{(\ell-2)!}{(\ell+2)!} \frac{(\ell+1+2m)y_{\ell m}^2}{2\ell+1} \frac{r_0^\ell}{r_1^{\ell+2}}. \tag{115}$$

We then repeat the conversion of the summation to a Taylor series, this time using the identity $b_{1/2}^{(m)}(\varsigma^{-1}) = \varsigma b_{1/2}^{(m)}(\varsigma)$ to relate the series in powers of r_0/r_1 to the Laplace coefficient at r_1/r_0. This gives

$$\begin{aligned} \mathcal{S}^{(m)} &= \frac{qM^{1/2}(\varsigma_m^+)^{1/2}}{2r_0^{1/2}} \Big[-\varsigma_m^+ b_{1/2}^{(m)\prime}(\varsigma_m^-) + 2m b_{1/2}^{(m)}(\varsigma_m^+) \\ &\quad -4(\varsigma_m^+)^{-2} b_{1/2}^{(1)\prime}(0)\delta_{m1} \Big], \end{aligned} \tag{116}$$

where the last term arises for $m = 1$ because the summation over modes begins at $\ell = 2$, whereas the Taylor series of $b_{1/2}^{(1)}$ has a first-order term, $b_{1/2}^{(1)\prime}(0) = 1$. This can be compared to the result for Paper I, where the last term was $-\varsigma_m^+\delta_{m1}$. The two terms are exactly equal at resonance $\varsigma_1^+ = 2^{2/3}$; recall that the resonance is however the only location where $\mathcal{S}^{(m)}$ is needed. Indeed, if one does a Newtonian calculation of $\mathcal{S}^{(m)}$ but working in the inertial frame (where the indirect term in the disturbing function is replaced by a term corresponding to the displacement of the primary), then one derives the last term in Eq. (116) in the form presented here. Of course, the two forms are equivalent on resonance as guaranteed by the gauge invariance arguments of Paper I.

7 RESONANCES IN THE SCHWARZSCHILD PROBLEM

We now come to our the first case where we explicitly compute angular momentum transport coefficients in a black hole spacetime: the Schwarzschild system. We first present the background coefficients and resonance locations, and then give the amplitudes. To simplify our expressions and avoid proliferation of "r/M", we will use units where the mass of the black hole is $M = 1$.

7.1 Circular orbits: a review

For circular orbits at radius r, the specific angular momentum and energy of a circular orbit are (Chandrasekhar 1992, §19$bi\alpha$)

$$\mathcal{L} = \frac{r}{\sqrt{r-3}} \quad \text{and} \quad \mathcal{E} = \frac{r-2}{\sqrt{r(r-3)}}. \tag{117}$$

Their derivatives are

$$\mathcal{L}' = \frac{r-6}{2(r-3)^{3/2}} \quad \text{and} \quad \mathcal{E}' = \frac{r-6}{2r^{3/2}(r-3)^{3/2}}. \tag{118}$$

The angular velocity is

$$\Omega = \frac{\mathcal{E}'}{\mathcal{L}'} = r^{-3/2}. \tag{119}$$

The conversion from proper to coordinate time is

$$w^t = \frac{\mathrm{d}t}{\mathrm{d}\tau} = \sqrt{\frac{r}{r-3}}. \tag{120}$$

The epicyclic frequency is

$$\kappa = \frac{\sqrt{r-6}}{r^2}, \tag{121}$$

and the specific epicyclic impedance is

$$\mathcal{Z} = \frac{1}{r-2}\sqrt{\frac{r-6}{r(r-3)}}. \tag{122}$$

We see that the epicyclic frequency and impedance both vanish at the ISCO $r = r_{\text{ISCO}} = 6$.

We now suppose that a perturber is placed on a circular equatorial orbit at radius $r_{\text{s}} > r_{\text{ISCO}} = 6$. Lindblad resonances of azimuthal quantum number m occur at

$$D(r) = m(r^{-3/2} - r_{\text{s}}^{-3/2}) \mp \frac{\sqrt{r-6}}{r^2} = 0. \tag{123}$$

There is no simple closed-form solution to this equation. However, we can deduce its properties by noting that

$$D'(r) = \frac{3}{2}r^{-5/2}\left[-m \pm \frac{r-8}{\sqrt{r(r-6)}}\right]. \tag{124}$$

Since $(r-8)/\sqrt{r(r-6)} < 1$, it follows that $D'(r) < 0$ for all positive m and $r > r_{\text{ISCO}}$. Thus we see that for each type of resonance (ILR or OLR) and for a given value of m, there is at most one solution to Eq. (123). Furthermore, we easily see that $D > 0$ for $r \approx r_{\text{ISCO}}$ and $D < 0$ at $r = \infty$, so there exists exactly one ILR and OLR for each positive integer m.

Here we note a key difference from the Keplerian case: there exists an $m = 1$ ILR. Ordinarily, the innermost Lindblad resonance is the $m = 2$ ILR (mean motion ratio 2:1), in which the test particle goes through two epicyclic periods in every synodic period. Due to pericentre precession, the Schwarzschild metric admits the $m = 1$ ILR, in which the orbital frequency of the perturber is equal to the pericentre precession frequency of the test particle. This is *not* a uniquely relativistic phenomenon, but can occur in any system whose attractive potential at small r exhibits a steeper than r^{-1} dependence, e.g. the potential in the equatorial plane of an oblate planet. Indeed, there is a ringlet of Saturn at 1.29 Saturn radii, whose pericentre precession rate nearly matches the orbital frequency of Titan, and which has thus acquired a large forced eccentricity (Porco et al. 1984).

7.2 Resonance strengths

We may now compute $\mathcal{S}^{(m)}$ by the method of Sec. 5 for each of the resonances. The first three ILRs are displayed in Figure 1, where we plot the resonance location r_1 as a function of the secondary location r_0; and also the torque strength with the perturbing mass and disk density normalized out,

$$N = \frac{T}{2\pi r_1 q^2 \Sigma(r_1)} = \mp \frac{\pi m w^t \mathcal{Z}}{|D'(r_1)|}|\mathcal{S}^{(m)}|^2. \tag{125}$$

The data are tabulated in Table 2.

The maximum value of ℓ used in the computation is a balance between computation time and overflow avoidance versus accuracy. At very large ℓ and small ω, the determination of e.g. $\aleph$ and c_{13} are susceptible to overflow due to the power-law behaviour with large indices ($r^{1-\ell}$ and $r^{2+\ell}$) of the radial solutions to the Teukolsky equation between

$r \sim 2$ and $r \sim \omega^{-1}$.[13] Fortunately, for the results in this paper we do not need to work in a regime where overflow occurs. For most cases, have used $\ell_{\max} = 20$ for the computations at $20 < r_0 \leqslant 250$ and $\ell_{\max} = 40$ at $8 \leqslant r_0 \leqslant 20$.[14] For the $m = 1$, 2, and 3 ILRs presented, we have estimated the truncation error in ℓ by extrapolating[15] the sequence of contributions from successive ℓ; such errors are found to be $\leqslant 0.1\%$ ($m = 1$ and $m = 2$) and $\leqslant 1\%$ ($m = 3$).

7.2.1 The $m \geqslant 2$ ILRs

For $m \geqslant 2$, this converges to a constant in the Keplerian limit,

$$\lim_{r_0 \to \infty} N = \mp \frac{\pi}{6} (\varsigma_m^-)^2 \left| \varsigma_m^- b_{1/2}^{(m)\prime}(\varsigma_m^-) + 2m b_{1/2}^{(m)}(\varsigma_m^-) \right|^2, \quad (126)$$

which is -2.36 for $m = 2$ and -7.50 for $m = 3$; the convergence can be seen from Fig. 1. As one moves inward toward the ISCO, the strength N increases; this is unsurprising since the resonance locations become closer to the secondary (in particular, as $r_0 \to r_{\text{ISCO}}$, we have $r_1/r_0 \to 1$).

7.2.2 The $m = 1$ ILR

For the $m = 1$ resonance, the strength is however much less, especially in the nearly Keplerian regime. This is in part due to the location of the resonance, with $r_1 \ll r_0$, and also due to the fact that the Newtonian quadrupole tidal field does not contribute to $\mathcal{S}^{(m)}$: reflection symmetry across the equatorial plane allows only $m \in \{-2, 0, 2\}$ contributions to the tidal field, and so the lowest-order contribution to the resonance strength comes from the (gravitoelectric) octupole ($\ell = 3$).

While the $m = 1$ ILR does not exist in the Keplerian problem, its location and strength may be estimated in the large-r_0 limit by post-Newtonian arguments. The location is determined by the condition that the precession rate,

$$\Omega - \kappa = \frac{\sqrt{r_1} - \sqrt{r_1 - 6}}{r_1^2} \approx \frac{3}{r_1^{5/2}}, \quad (127)$$

correspond to the secondary orbital angular velocity, $r_0^{-3/2}$. This implies, for large r_0,

$$r_1 \approx 3^{2/5} r_0^{3/5} \approx 1.55 r_0^{3/5}. \quad (128)$$

The strength of the resonance in the large-r_0 limit can be estimated from Eq. (110); the leading-order term is $\ell = 3$, which gives

$$\mathcal{S}^{(1)} \approx 4.36 r_0^{-19/10} \quad \text{and} \quad N \approx -19.2 r_0^{-13/5}. \quad (129)$$

---

[13] In principle such errors could be removed by working with $\ln \mathcal{R}(r)$ instead of $\mathcal{R}(r)$, but we have not done this as it would have resulted in much more complex code (including branching to avoid numerical instabilities when $\mathcal{R}$ passes near zero). An alternative would have been to define a new floating-type data type with more bits in the exponent.

[14] The exceptions are that for $20 < r_0 \leqslant 40$ we use $\ell_{\max} = 40$ for the $m = 3$ ILRs; and for $r_0 > 20$ we use $\ell_{\max} = 30$ for the $m = 2$ OLRs.

[15] Since there is a strong odd-even pattern to the contributions from successive multipoles, we used the last two even ℓs to generate a geometric sequence of even ℓs and did a similar independent procedure for the odd ℓs.

This result is valid at very large r. However, at even modest r it substantially overestimates the strength of the $m = 1$ resonance: the true N is smaller by a factor of 0.75 at $r_0 = 250$ and 0.66 at $r_0 = 50$. The principal reason is that there is another contribution to $\mathcal{P}^{(1)}$ from the gravitomagnetic quadrupole mode ($\ell = 2$, negative parity), which does not exist in the Newtonian theory but has the correct symmetry properties for two equatorial orbits to interact via an $m = 1$ mode. Roughly speaking, the gravitomagnetic interaction should give a contribution to $\mathcal{S}^{(1)}$ that is suppressed by the product of the orbital velocities $v_0 v_1 \sim r_0^{-1/2} r_1^{-1/2} \sim r_0^{-4/5}$, but (due to the angular momentum barrier for $\ell = 2$ versus 3) enhanced relative to the gravitoelectric octupole by a factor of $(r_1/r_0)^{-1} \sim r_0^{2/5}$. Thus overall, the gravitomagnetic quadrupole interaction is only weaker than the gravitoelectric octupole by a factor of $\sim r_0^{-2/5}$. It turns out that the two contributions to $\mathcal{S}^{(1)}$ have opposite sign, resulting in a suppression of the $m = 1$ ILR strength. The correction is not small:

$$\frac{\mathcal{S}^{(1)}(\text{magnetic quadrupole})}{\mathcal{S}^{(1)}(\text{electric octupole})} = \begin{cases} -0.19, & r_0 = 250 \\ -0.38, & r_0 = 50, \end{cases} \quad (130)$$

and then the resonant torque depends on the square of $\mathcal{S}^{(m)}$ so these corrections are effectively doubled.

The reason for the opposite sign of the gravitomagnetic quadrupole contribution can be understood from linearized gravity arguments. To lowest order, a moving particle in the vicinity of a moving perturber experiences a gravitomagnetic "acceleration" (Wald 1984, §4.4a):

$$\boldsymbol{a} = -4\boldsymbol{v} \times \boldsymbol{B}, \quad \boldsymbol{B}(\boldsymbol{r}) = qM\boldsymbol{v}_0 \times \frac{\boldsymbol{r} - \boldsymbol{r}_0}{|\boldsymbol{r} - \boldsymbol{r}_0|^3}, \quad (131)$$

i.e. $\boldsymbol{B}$ is the field generated from the momentum in the same way that a magnetic field is generated by electric current. Here $\boldsymbol{r}_0$ is the position of the perturber and $\boldsymbol{v}_0$ is its velocity. The test particle experiences an inward gravitomagnetic acceleration that is strongest at inferior conjunction (i.e. when the longitudes of the test particle and perturber are equal). This is the opposite of the Newtonian gravitoelectric octupole field, which produces an outward force at inferior conjunction.

7.2.3 The OLRs

The outer Lindblad resonances, being external to the perturber, are more similar to their Keplerian counterparts than the inner Lindblad resonances. The limiting strengths as $r_0 \to \infty$ for the $m = 1$ (2:1) and $m = 2$ (3:2) OLRs are $N = 0.19$ and $N = 8.62$ respectively; their behaviour at smaller radii is shown in Table 2.

For the strong $m = 2$ OLR, the resonant strength increases as we move inward because the Lindblad resonances are closer to the perturber than they are in the Keplerian case. However, the weaker $m = 1$ OLR (2:1) suffers from the same partial cancellation of gravitoelectric octupole and gravitomagnetic quadrupole contributions as the $m = 1$ ILR. Therefore at small radii it actually becomes weaker.

8 RESONANCES IN THE KERR PROBLEM

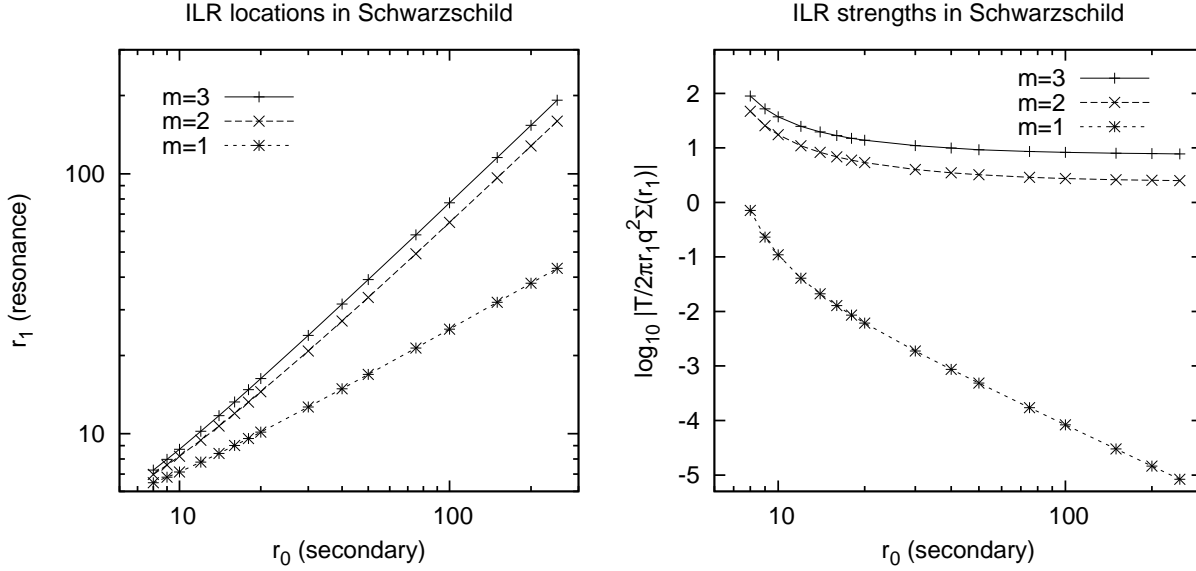We may now move on to the resonances associated with the circular, equatorial orbits in the Kerr spacetime. Again,

ILR locations in Schwarzschild

ILR strengths in Schwarzschild

Figure 1. The locations and strengths of the inner Lindblad resonances in the Schwarzschild spacetime. The $m \geqslant 2$ resonances have Keplerian analogues; their strength in these units approaches a constant in the Keplerian regime, but grows as one approaches the ISCO. The $m = 1$ resonance exists only due to the pericentre precession, and is found at much smaller radius; it is also much weaker, although its strength grows as we move inward.

Table 2. The resonant strengths in the Schwarzschild problem for $m = 1$ and $m = 2$ Lindblad resonances; here r_0 is the orbital radius of the perturber and r_1 is the resonance location. Truncation errors due to choice of $\ell_{\max}$ are estimated to be $\leqslant 0.1\%$ for the cases given in the table.

| | $m = 1$ ILR (0:1) | | $m = 2$ ILR (1:2) | | $m = 2$ OLR (3:2) | | $m = 1$ OLR (2:1) | |
r_0	r_1	N	r_1	N	r_1	N	r_1	N
8.00	6.48	$-7.11\text{E}-1$	6.97	$-4.69\text{E}+1$	9.55	$+2.28\text{E}+1$	11.33	$+7.05\text{E}-2$
9.00	6.80	$-2.32\text{E}-1$	7.57	$-2.55\text{E}+1$	10.91	$+1.79\text{E}+1$	12.99	$+8.76\text{E}-2$
10.00	7.13	$-1.10\text{E}-1$	8.19	$-1.74\text{E}+1$	12.26	$+1.51\text{E}+1$	14.62	$+1.01\text{E}-1$
12.00	7.78	$-4.08\text{E}-2$	9.44	$-1.09\text{E}+1$	14.92	$+1.30\text{E}+1$	17.85	$+1.19\text{E}-1$
14.00	8.40	$-2.10\text{E}-2$	10.70	$-8.27\text{E}+0$	17.57	$+1.18\text{E}+1$	21.07	$+1.31\text{E}-1$
16.00	9.01	$-1.28\text{E}-2$	11.97	$-6.85\text{E}+0$	20.21	$+1.11\text{E}+1$	24.26	$+1.40\text{E}-1$
18.00	9.58	$-8.57\text{E}-3$	13.23	$-5.96\text{E}+0$	22.84	$+1.07\text{E}+1$	27.46	$+1.46\text{E}-1$
20.00	10.14	$-6.12\text{E}-3$	14.50	$-5.37\text{E}+0$	25.47	$+1.04\text{E}+1$	30.65	$+1.51\text{E}-1$
30.00	12.67	$-1.89\text{E}-3$	20.82	$-4.00\text{E}+0$	38.60	$+9.60\text{E}+0$	46.56	$+1.66\text{E}-1$
40.00	14.89	$-8.69\text{E}-4$	27.13	$-3.49\text{E}+0$	51.72	$+9.30\text{E}+0$	62.45	$+1.73\text{E}-1$
50.00	16.91	$-4.86\text{E}-4$	33.44	$-3.22\text{E}+0$	64.83	$+9.13\text{E}+0$	78.33	$+1.77\text{E}-1$
75.00	21.36	$-1.72\text{E}-4$	49.21	$-2.89\text{E}+0$	97.59	$+8.94\text{E}+0$	118.03	$+1.82\text{E}-1$
100.00	25.25	$-8.33\text{E}-5$	64.97	$-2.75\text{E}+0$	130.36	$+8.85\text{E}+0$	157.72	$+1.85\text{E}-1$
150.00	32.00	$-3.01\text{E}-5$	96.47	$-2.61\text{E}+0$	195.88	$+8.77\text{E}+0$	237.10	$+1.87\text{E}-1$
200.00	37.91	$-1.46\text{E}-5$	127.98	$-2.54\text{E}+0$	261.40	$+8.73\text{E}+0$	316.47	$+1.88\text{E}-1$
250.00	43.25	$-8.35\text{E}-6$	159.48	$-2.50\text{E}+0$	326.92	$+8.70\text{E}+0$	395.84	$+1.89\text{E}-1$

we use units where the mass of the primary hole $M = 1$, and hence $a = a_\star$. We consider prograde orbits, and use $a < 0$ to represent retrograde orbits. The machinery we have developed in the previous sections is completely general and may be used to compute resonance strengths in Kerr with no new difficulties.

The problem is very similar to that of the Schwarzschild spacetime: there exists an ISCO at which $\kappa \to 0$, and hence once again there exists an $m = 1$ ILR. This time the basic

frequencies are

$$\Omega = \frac{1}{r^{3/2} + a} \quad \text{and} \quad \kappa = \Omega\sqrt{1 - \frac{6}{r} + \frac{8a}{r^{3/2}} - \frac{3a^2}{r^2}} \quad (132)$$

(Okazaki et al. 1987, Appendix). The sign of the a term in κ/Ω implies that pericentre precession is enhanced for $a < 0$ (the same effect is responsible for the larger r_{ISCO}). Thus we expect that the $m = 1$ ILR, which owes its existence to pericentre precession, will be stronger for retrograde orbits. This is indeed the case; in Fig. 2, we show the locations and strengths of the $m = 1$ ILR as a function of the secondary radius r_0. The behaviour of each resonance as a function of

the black hole spin at fixed $r_0 = 50$ is shown in Fig. 3; here we see that, as expected, the $m = 1$ ILR is most affected: the difference between near-maximal prograde and retrograde spins ($a_\star = \pm 0.95$) is a factor of 6 in the resonance strength. However, in all cases the $m = 1$ ILR is much weaker than the $m \geqslant 2$ ILRs.

9   DISCUSSION

The Newtonian formulae for the torque applied to a disc at the Lindblad resonances associated with a perturber on a circular equatorial orbit have been extended into the relativistic regime. The calculation has revealed both new physical effects, and has provided a mathematical connection between seemingly disparate phenomena: resonant torques and gravitational radiation.

At the *physical* level, we have learned that relativistic effects introduce an additional $m = 1$ inner Lindblad resonance at which the pericentre precession rate of the test particle matches the pattern speed of the perturbation. This has no Keplerian analogue, but in quasi-Newtonian language one can think of it as being due to the steepening of the potential. Indeed, any Newtonian potential with an ISCO will have this resonance. We found, however, that the quasi-Newtonian calculation of the resonant strength, which is due to the tidal octupole, is suppressed by tens of percents due to gravitomagnetic corrections even at $r_0/M > 100$. In this sense the $m = 1$ ILR is a relativistic beast.

At the *mathematical* level, our method of computation has revealed a connection between, on the one hand, angular momentum transfer via the Lindblad resonances; and on the other hand, the product of the gravitational wave signals emitted to infinity and into the hole by the perturber and the test particle (assuming the latter to be in an orbit of infinitesimal eccentricity). This connection arose from general principles: (i) the conservation of energy and angular momentum when the contribution to both from gravitational waves is included; (ii) the fact that, aside from the $\ell = 0$ and 1 modes that do not contribute to resonant transfer, the entire perturbed spacetime structure in the vacuum regions is determined by the radiation degrees of freedom, described for Type D spacetimes by ψ_4; and (iii) the ability to describe epicyclic motion of the test particle via Hamiltonian dynamics. This was not expected when we began the calculation, and we are still lacking an intuitive explanation.

REFERENCES

Abramowitz M., Stegun I., 1972, Handbook of Mathematical Functions, Dover, New York, NY

Arnold V., 1978, Mathematical Methods of Classical Mechanics, Springer, New York, NY

Boyer R., Lindquist R., 1967, J. Math. Phys., 8, 265

Chandrasekhar S., 1992, The Mathematical Theory of Black Holes, Oxford University Press, New York, NY

Chang P., Strubbe L., Menou K., Quataert E., 2010, MNRAS, 407, 2007

Chrzanowski P., 1975, Phys. Rev. D, 11, 2042

Detweiler S., 1978, ApJ, 225, 687

Drasco S., Hughes S., 2006, Phys. Rev. D, 73, 024027

Drasco S., Flanagan É., Hughes S., 2005, Cl. Quant. Grav., 22, S801

Flanagan É., Hinderer T., 2010, preprint, arXiv:1009.4923

Goldberg J., Macfarlane A., Newman E., Rohrlich F., Sudarshan E., 1967, J. Math. Phys., 8, 2155

Goldreich P., Tremaine S., 1978, ApJ, 222, 850

Goldreich P., Tremaine S., 1979, ApJ, 233, 857

Goldreich P., Tremaine S., 1980, ApJ, 241, 425

Goldstein H., Poole C., Safko J., 2002, Classical Mechanics, 3rd ed., Addison-Wesley, San Francisco, USA

Hinderer T., Flanagan É., 2008, Phys. Rev. D, 78, 064028

Hughes S., 2000, Phys. Rev. D, 61, 084004

Hughes S., Drasco S., Flanagan É., Franklin J., 2005, Phys. Rev. Lett., 04, 221101

Kennefick D., 1998, Phys. Rev. D, 58, 064012

Lin D., Papaploizou J., 1979, MNRAS, 186, 799

Lynden-Bell D., Kalnajs A., 1972, MNRAS, 157, 1

Mano S., Suzuki H., Takasugi E., 1996, Prog. Theor. Phys., 95, 1079

Mino Y., Sasaki M., Shibata M., Tagoshi H., Tanaka T., 1997, Prog. Theor. Phys. Supp., 128, 1

Mino Y., 2003, Phys. Rev. D, 67, 084027

Misner C., Thorne K., Wheeler J., 1973, Gravitation, W. H. Freeman and Co., San Francisco, California, USA

Murray C., Dermott S., 2000, Solar System Dynamics, Cambridge University Press, Cambridge, UK

Newman E., Penrose R., 1966, J. Math. Phys., 7, 863

Okazaki A., Kato S., Fukue J., 1987, PASJ, 39, 457

Ori A., 2003, Phys. Rev. D, 67, 124010

Porco C., Nicholson P., Borderies N., Danielson G., Goldreich P., Holberg J., Lane A., 1984, Icarus, 60, 1

Press W., Teukolsky S., 1973, ApJ, 185, 649

Press W., Teukolsky S., Vetterling W., Flannery B., 1992, Numerical recipes in C. The art of scientific computing, Cambridge University Press, Cambridge, UK

Sasaki M., Nakamura T., 1982a, Phys. Lett. A, 89, 68

Sasaki M., Nakamura T., 1982b, Prog. Theor. Phys., 67, 1788

Sasaki M., Tagoshi H., 2003, Living Reviews in Relativity, 6, 6

Schmidt W., 2002, Cl. Quant. Grav., 19, 2743

Shibata M., 1993, Phys. Rev. D, 48, 663

Shibata M., 1994, Phys. Rev. D, 50, 6297

Teukolsky S., 1973, ApJ, 185, 635

Teukolsky S., Press W., 1974, ApJ, 193, 443

Wald R., 1978, Phys. Rev. Lett., 41, 203

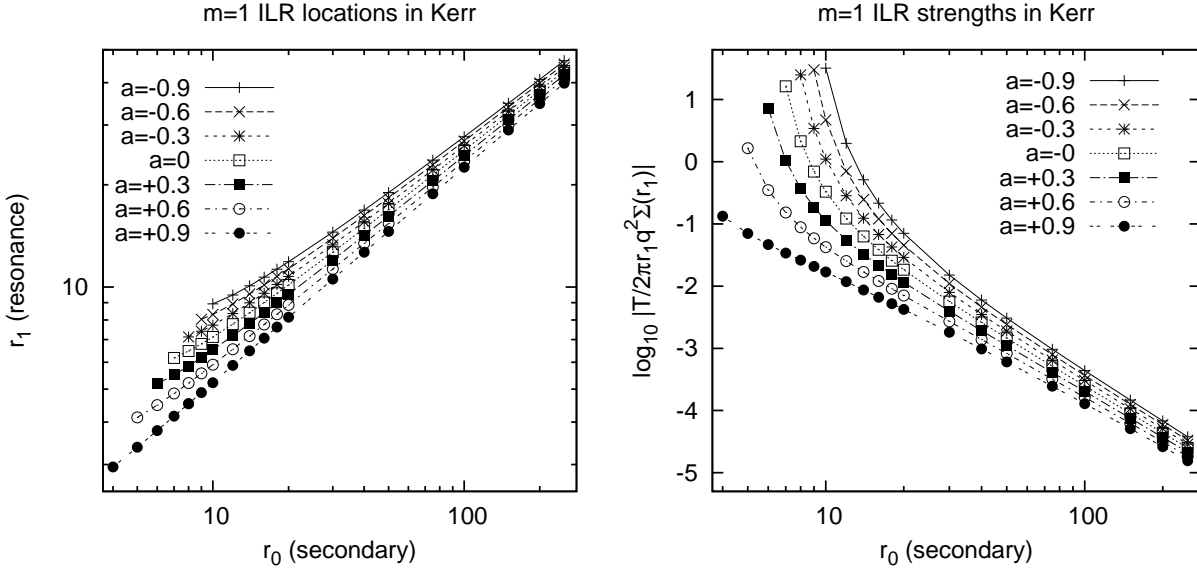Wald R., 1984, General Relativity, University of Chicago Press, Chicago, IL

Figure 2. The locations and strengths of the $m = 1$ ILR for equatorial orbits in the Kerr spacetime. For prograde orbits ($a > 0$) the resonance moves inward and become weaker, whereas for retrograde orbits the resonance moves outward and becomes stronger.
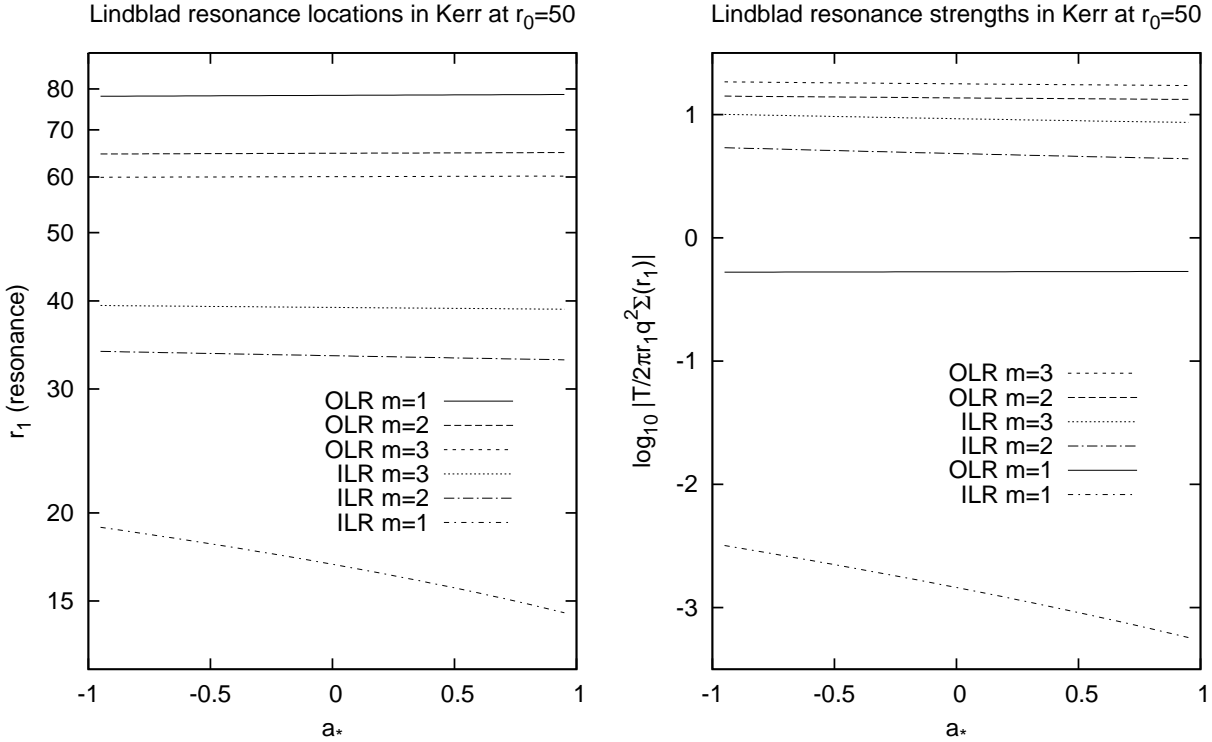

Figure 3. The locations and strengths of the Lindblad resonances as a function of black hole spin for a perturber in a circular orbit at $r_0 = 50M$.

APPENDIX A: SPHEROIDAL HARMONICS

This appendix considers the solution to the angular eigen-mode equation, Eq. (44), for $S_{\ell,m}^{s,\chi}(\theta)$.

The most convenient way to solve Eq. (44) is to write the eigenfunctions as linear combinations of the spin-weighted spherical harmonics (Newman & Penrose 1966; Goldberg et al. 1967), as has been done in previous works (e.g. Press & Teukolsky 1973; Hughes 2000)

$$S_{\ell,m}^{\chi}(\theta) = \sum_{j=\max(|m|,|s|)}^{\infty} b_{j\ell m}(\chi) Y_{\ell,m}^s(\theta), \qquad (A1)$$

where the coefficients $b_{j\ell m}(\chi)$ satisfy the eigenvalue equation (Press & Teukolsky 1973, §IIIa),

$$\mathbf{C}b = \mathcal{E}_{\ell,m}^s b, \tag{A2}$$

where b is a vector of length $j_{\max} - j_{\min} + 1$ where $j_{\min} = \ell_{\min}$ and $j_{\max}$ is the highest angular momentum harmonic used in the finite basis set. The matrix $\mathbf{C}$ is real and symmetric, and is band-diagonal in the sense that $C_{jj'} = 0$ if $|j - j'| > 2$ (Press & Teukolsky 1973). In numerical computation, we truncate at $j_{\max}$, obtain the eigenvalues $\mathcal{E}_{\ell,m}^s$ and eigenvectors b by Jacobi iteration, and compute the residual

$$e = \sqrt{\sum_{j > j_{\max}} (\mathbf{C}b)_j^2}; \tag{A3}$$

$j_{\max}$ is increased until e falls below some error threshold (usually 10^{-8}) for all desired ℓ. The eigenvectors are normalized using $\sum_j b_{j\ell m}^2 = 2\pi$, which is equivalent to the usual normalization,

$$\int_0^\pi \sin\theta \left| S_{\ell,m}^{s,\chi}(\theta) \right|^2 d\theta = 1. \tag{A4}$$

The spin-weighted spherical harmonics are computed directly from the rotation matrices,

$$Y_{\ell,m}^s(\theta) = (-1)^m [\mathbf{D}(\theta)]_{-s,m} = (-1)^m [\exp(\mathrm{i}\theta \mathbf{L}_2)]_{-s,m}, \tag{A5}$$

where $\mathbf{L}_2$ is the angular momentum operator around the 2-axis in the spin-ℓ representation of SO(3).[16] The complex exponential is computed by a quadratic expansion for small θ ($\theta < 10^{-8}$), and for larger values by repeated squaring of the rotation matrix $\mathbf{D}(\theta)$ (each squaring doubles θ). For this process, we actually store $\mathbf{D}(\theta) - \mathbf{1}$ where $\mathbf{1}$ is the $(2\ell + 1) \times (2\ell + 1)$ identity matrix; this is numerically preferable for small θ to avoid exponential amplification of rounding errors in the squaring process. The squaring process is then

$$\mathbf{D}(2\theta) - \mathbf{1} = 2[\mathbf{D}(\theta) - \mathbf{1}] + [\mathbf{D}(\theta) - \mathbf{1}]^2. \tag{A6}$$

This method is slow but is stable, simple to code, and does not suffer from underflow occurrences (common in many publicly available spherical harmonics routines even at modest ℓ). It also returns estimates of the θ-derivatives with no extra effort since

$$\frac{d\mathbf{D}(\theta)}{d\theta} = \mathrm{i}\mathbf{L}_2 \mathbf{D}(\theta). \tag{A7}$$

For evaluation of the source terms, we require $\mathbb{L}_2^\dagger S$ and $\mathbb{L}_1^\dagger \mathbb{L}_2^\dagger S$. Given S and $\partial_\theta S$, it is easy to compute

$$\mathbb{L}_2^\dagger S = \partial_\theta S + (-m\csc\theta + \chi\sin\theta + 2\cot\theta)S. \tag{A8}$$

We further see that

$$\begin{aligned}
\mathbb{L}_1^\dagger \mathbb{L}_2^\dagger S = {}& \partial_\theta^2 S + (-2m\csc\theta + 2\chi\sin\theta + 3\cot\theta)\partial_\theta S \\
& + (m^2\csc^2\theta + \chi^2\sin^2\theta - 2 - 2m\chi \\
& - 2m\csc\theta\cot\theta + 4\chi\cos\theta)S.
\end{aligned} \tag{A9}$$

We may now use the angular Teukolsky equation for S,

---

[16] With the standard (Condon-Shortley) phases, $\mathrm{i}\mathbf{L}_2$ is real and antisymmetric.

© 0000 RAS, MNRAS **000**, 000–000

which is a second-order ODE that expresses $\partial_\theta^2 S$ in terms of S, $\partial_\theta S$, and the eigenvalue $\mathcal{E}$. Substituting out $\partial_\theta^2 S$, we find

$$\begin{aligned}
\mathbb{L}_1^\dagger \mathbb{L}_2^\dagger S = {}& 2(-m\csc\theta + \chi\sin\theta + \cot\theta)\partial_\theta S \\
& + [-\chi^2\cos 2\theta - 2m\chi + 2m^2\csc^2\theta \\
& - 6m\csc\theta\cot\theta - 2 + 4\csc^2\theta - \mathcal{E}]S,
\end{aligned} \tag{A10}$$

which is the form we use.

APPENDIX B: SCATTERING MATRIX

Here we concern ourselves with the scattering matrix relating the four solutions of the radial Teukolsky equation,

$$\begin{pmatrix} \mathcal{R}_1(r) \\ \mathcal{R}_2(r) \end{pmatrix} = \begin{pmatrix} c_{13} & c_{14} \\ c_{23} & c_{24} \end{pmatrix} \begin{pmatrix} \mathcal{R}_3(r) \\ \mathcal{R}_4(r) \end{pmatrix}, \tag{B1}$$

where the c_{ab} are 4 complex coefficients that we wish to compute. (We may also want the inverse matrix.) Our goal here is the numerical computation of the c_{ab} coefficients analytically from $\aleph$ and the parameters of the problem.

The Wronskian of any two solutions is $W_{ab} = \mathcal{R}_a \mathcal{R}_b' - \mathcal{R}_b \mathcal{R}_a'$ and is proportional to Δ. In particular, the asymptotic solutions give at the horizon gives

$$W_{12} = 2(\mathrm{i}\varpi - \Gamma)\frac{dr_\star}{dr}\bigg|_{r_{\mathrm{h}+}} \Delta^2 = 2\beta\Delta, \tag{B2}$$

where

$$\beta \equiv 2\mathrm{i}Mr_{\mathrm{h}+}\omega - \mathrm{i}am - 2\sqrt{M^2 - a^2}. \tag{B3}$$

The solutions at large radius give $W_{34} = -2\mathrm{i}\omega\Delta$. We have also set $W_{31} = \aleph\Delta$.

The above Wronskian elements constrain the c_{ab}. First, Eq. (B1) sets W_{12} equal to W_{34} times the determinant of the matrix of c_{ab}, so:

$$c_{13}c_{24} - c_{14}c_{23} = \mathrm{i}\frac{\beta}{\omega}. \tag{B4}$$

Second, the definition of $\aleph$ implies that $\aleph\Delta = -c_{14}W_{34}$, so

$$c_{14} = -\mathrm{i}\frac{\aleph}{2\omega}. \tag{B5}$$

Further relations can be found from considering the conservation of energy. For a general case with

$$\mathcal{R}(r) = b_1 \mathcal{R}_1(r) + b_2 \mathcal{R}_2(r) = b_3 \mathcal{R}_3(r) + b_4 \mathcal{R}_4(r), \tag{B6}$$

the conservation of energy (Teukolsky & Press 1974) then provides the relation

$$|b_3|^2 + \alpha|b_1|^2 = \frac{(2\omega)^8}{|C|^2}|b_4|^2 + \alpha_2|b_2|^2. \tag{B7}$$

Here the b_2 term denotes power emerging from the past horizon, whose value is not required here. This relation may be evaluated for the case of $\mathcal{R} = \mathcal{R}_1 + \sigma\mathcal{R}_2$; equating terms on both sides proportional to 1 and σ (or σ^*) gives respectively

$$|c_{13}|^2 + \alpha = \frac{(2\omega)^6}{|C|^2}|\aleph|^2 \tag{B8}$$

and

$$c_{23}^* c_{13} = \frac{(2\omega)^8}{|C|^2} c_{24}^* c_{14}. \tag{B9}$$

Equation (B9) enables us to solve for c_{23} in terms of the

other coefficients; substituting into the determinant relation, Eq. (B4), eliminates c_{23} and generates a linear equation for c_{24} in terms of c_{13} and c_{14}:

$$\left[-\frac{(2\omega)^8 c_{14}^*}{|C|^2 c_{13}^*} c_{14} + c_{13} \right] c_{24} = \mathrm{i}\frac{\beta}{\omega}. \qquad (B10)$$

Using Eq. (B8) and substituting for c_{14} (from Eq. B5) simplifies this to

$$c_{24} = -\frac{\mathrm{i}\beta c_{13}^*}{\alpha\omega}, \qquad (B11)$$

and hence

$$c_{23} = -\frac{\mathrm{i}\beta}{\alpha\omega}\frac{(2\omega)^8}{|C|^2} c_{14}^*. \qquad (B12)$$

The programme to compute the c_{ab} is thus as follows:

• First obtain c_{14} from Eq. (B5) and the solution for $\aleph$ from Sec. 4.4.
• Next obtain c_{13} by integrating the $\mathcal{R}_1$ solution along the real axis to large r, where the $\mathcal{R}_3$ solution becomes dominant. By dividing by the asymptotic form for $\mathcal{R}_3$ (again keeping the first two coefficients in the expansion), obtain the coefficient of $\mathcal{R}_3$ in $\mathcal{R}_1$, i.e.c_{13}.
• Evaluate β and then use Eqs. (B11) and (B12) to obtain c_{24} and c_{23}.

The inverse transformation coefficients c_{31}, c_{32}, c_{41}, and c_{42} can be obtained in accordance with

$$\left(\begin{array}{cc} c_{31} & c_{32} \\ c_{41} & c_{42} \end{array} \right) = \frac{\omega}{\mathrm{i}\beta} \left(\begin{array}{cc} c_{24} & -c_{14} \\ -c_{23} & c_{13} \end{array} \right); \qquad (B13)$$

we note that the substitution of the formula for the determinant in the denominator is required if this relation is used for numerical computation because of the very large correlation coefficient of the matrix, i.e. for some practical cases we have $c_{13}c_{24} \approx c_{14}c_{23}$. However, for formulas involving c_{31} it is more convenient to combine this with Eq. (B11) to obtain

$$c_{31} = -\frac{c_{13}^*}{\alpha}. \qquad (B14)$$

APPENDIX C: RADIAL MODES AT LOW FREQUENCY

This appendix describes the radial modes in the nonrelativistic regime, i.e. where $\omega \ll M^{-1}$ and $M \ll r \ll \omega^{-1}$. This is the regime relevant for Keplerian discs (Section 6). The angular modes simply reduce to spin-weighted spherical harmonics with separation constant $\mathcal{E} = \ell(\ell+1)$.

There are infinite (logarithmically divergent in r or $r - r_{h+}$) phase errors in our approximations here; this does not concern us since the absolute phases of $\mathcal{R}_1$ at the horizon or $\mathcal{R}_3$ at infinity cancel out of the computation.

The solution of the radial modes in terms of $_1F_1$ functions is described in greater generality by Mano et al. (1996); see also the review by Sasaki & Tagoshi (2003, §4). We sketch here a simplified derivation for the specialized case of small ω, which does not require a "renormalized angular momentum parameter" and has much shorter expressions.

C1   The $\mathcal{R}_1$ solution

The $\mathcal{R}_1$ solution (no radiation emerging from the past horizon) in this regime can be constructed by taking $\omega \to 0$. With this simplification, the radial Teukolsky equation can be reduced to a hypergeometric equation (Mano et al. 1996). The solution is

$$\mathcal{R} \propto (-x)^{2-\mathrm{i}\tau/2}(1-x)^{-\mathrm{i}\tau/2}\,_2F_1(\ell+1-\mathrm{i}\tau, -\ell-\mathrm{i}\tau; 3-\mathrm{i}\tau; x), \qquad (C1)$$

where

$$x = \frac{r_{h+} - r}{r_{h+} - r_{h-}} = -\frac{r - r_{h+}}{2\sqrt{M^2 - a^2}} \qquad (C2)$$

and $\tau = -am/\sqrt{M^2 - a^2}$. We note that in the relevant regime $x < 0$, and take the branch $\arg(1-x) = \arg(-x) = 0$ of the fractional powers.

The normalization of $\mathcal{R}_1$ can be obtained by taking the limit as $r \to r_{h+}^+$ ($-x \to 0^+$). This gives

$$\mathcal{R}_1 \to \Delta^2 \mathrm{e}^{\mathrm{i}m\Omega_H r_\star} \approx 16(M^2 - a^2)^2 \mathrm{e}^{\mathrm{i}m\varphi_0}(-x)^{2-\mathrm{i}\tau/2}, \quad (C3)$$

where $\varphi_0 = \frac{1}{2}a_\star + \Omega_H M \ln(1 - a_\star^2)$ and we have substituted for Ω_H in order to simplify the exponent of $-x$. We thus see that

$$\lim_{\omega\to 0}\mathcal{R}_1(r) = 16(M^2 - a^2)^2 \mathrm{e}^{\mathrm{i}m\varphi_0}(-x)^{2-\mathrm{i}\tau/2}(1-x)^{-\mathrm{i}\tau/2}$$
$$\times\,_2F_1(\ell+1-\mathrm{i}\tau, -\ell-\mathrm{i}\tau; 3-\mathrm{i}\tau; x). \quad (C4)$$

The series can be made finite using the linear transformation formula (Abramowitz & Stegun 1972, Eq. 15.3.3):

$$\lim_{\omega\to 0}\mathcal{R}_1(r) = 16(M^2 - a^2)^2 \mathrm{e}^{\mathrm{i}m\varphi_0}(-x)^{2-\mathrm{i}\tau/2}(1-x)^{2+\mathrm{i}\tau/2}$$
$$\times\,_2F_1(2-\ell, 3+\ell; 3-\mathrm{i}\tau; x). \quad (C5)$$

To reach the Keplerian regime, we must follow this to the regime where $-x \gg 1$. Taking the highest-order ($r^{\ell-2}$) term in the series, we find

$$\mathcal{R}_1(r) \approx -16(M^2 - a^2)^2 \mathrm{e}^{\mathrm{i}m\varphi_0}\frac{(2\ell)!}{(\ell+2)!}\frac{\Gamma(3-\mathrm{i}\tau)}{\Gamma(\ell+1-\mathrm{i}\tau)}$$
$$\times\left(\frac{r}{2\sqrt{M^2 - a^2}}\right)^{\ell+2}. \quad (C6)$$

For our purposes, this may be written as

$$\mathcal{R}_1(r) \to k_1 r^{\ell+2}, \qquad (C7)$$

where using the recursion relation for the Γ function[17],

$$|k_1| = [2(M^2 - a^2)]^{(2-\ell)/2}\frac{(2\ell)!}{(\ell+2)!}\left[\prod_{n=3}^{\ell}(n^2 + \tau^2)\right]^{-1/2}. \qquad (C8)$$

We will not require the *phase* of k_1; indeed, the phase is meaningless at the level of approximation here because in taking $\omega \to 0$ we introduce a phase error of $\sim \omega|r_\star|$, which diverges as one approaches the horizon.

C2   The $\mathcal{R}_3$ solution

We are now interested in the solutions that asymptote to a purely outgoing wave at $r \to \infty$. In this case, we keep ω but

---

[17] The product is empty for $\ell = 2$, in which case it is understood to evaluate to unity.

approximate $M, a \to 0$. Mano et al. (1996) also provides a solution in this case in terms of a confluent hypergeometric function. They find $\mathcal{R} \propto rf$, where $z = \omega r$ and $f(z)$ satisfies the relation

$$z^2 \frac{\mathrm{d}^2 f}{\mathrm{d}z^2} + [z^2 - 4\mathrm{i}z - \ell(\ell + 1)]f = 0. \qquad \text{(C9)}$$

As is well-known, this equation reduces to a $_1F_1$-type series upon the substitution $f(z) = \mathrm{e}^{\pm \mathrm{i}z}g(z)$. Four solutions may be obtained this way, depending on the chosen leading power of z:

$$
\begin{aligned}
\mathcal{R}_{\mathrm{A}}(r) &= r^{\ell+2}\mathrm{e}^{-\mathrm{i}\omega r}\,_1F_1(\ell + 3; 2\ell + 2; 2\mathrm{i}\omega r), \\
\mathcal{R}_{\mathrm{B}}(r) &= r^{1-\ell}\mathrm{e}^{-\mathrm{i}\omega r}\,_1F_1(2 - \ell; -2\ell; 2\mathrm{i}\omega r), \\
\mathcal{R}_{\mathrm{C}}(r) &= r^{\ell+2}\mathrm{e}^{\mathrm{i}\omega r}\,_1F_1(\ell - 1; 2\ell + 2; -2\mathrm{i}\omega r), \quad \text{and} \\
\mathcal{R}_{\mathrm{D}}(r) &= r^{1-\ell}\mathrm{e}^{\mathrm{i}\omega r}\,_1F_1(-2 - \ell; -2\ell; -2\mathrm{i}\omega r). \qquad \text{(C10)}
\end{aligned}
$$

Of these, $\mathcal{R}_{\mathrm{B}}$ and $\mathcal{R}_{\mathrm{D}}$ have the advantage of having truncating (polynomial) $_1F_1$ series; due to the nature of their oscillating parts they are manifestly linearly independent and provide a complete basis. The highest power in r shows that $\mathcal{R}_{\mathrm{B}}(z)$ yields the $\mathcal{R}_4$ solution and $\mathcal{R}_{\mathrm{D}}(z)$ yields the R_3 solution. The normalization is easily obtained from the highest term:

$$\mathcal{R}_3(r) = \mathrm{i}^{\ell-2}\frac{(2\ell)!\,r^{1-\ell}\mathrm{e}^{\mathrm{i}\omega r}}{(\ell - 2)!\,(2\omega)^{\ell+2}}\,_1F_1(-2 - \ell; -2\ell; -2\mathrm{i}\omega r). \qquad \text{(C11)}$$

This is only valid in the limiting case where $M \to 0$; finite mass introduces a logarithmically divergent phase error due to the long-range nature of the background metric perturbation (the asymptotic expansion of $\mathrm{d}r_\star/\mathrm{d}r - 1$ begins with the order r^{-1} term).

For Keplerian problems, we require the near-field solution $r \ll \omega^{-1}$, where

$$\mathcal{R}_3(r) = k_3 r^{1-\ell} \qquad \text{(C12)}$$

with

$$k_3 = \mathrm{i}^{\ell-2}\frac{(2\ell)!}{(\ell - 2)!\,(2\omega)^{\ell+2}}. \qquad \text{(C13)}$$

A similar result allows us to normalize $\mathcal{R}_4$: in the near-field zone, $\mathcal{R}_4(r) = k_4 r^{1-\ell}$ with

$$k_4 = \mathrm{i}^{-\ell-2}\frac{(2\ell)!}{(\ell + 2)!}(2\omega)^{2-\ell}. \qquad \text{(C14)}$$

C3 Wronskians and scattering coefficients

The Wronksian of the $\mathcal{R}_1$ and $\mathcal{R}_3$ solutions is easily evaluated in the Keplerian range of radii. It leads to $\aleph = (2\ell + 1)k_1 k_3$, hence

$$\aleph = \mathrm{i}^{\ell-2}\frac{(2\ell + 1)!}{(\ell - 2)!\,(2\omega)^{\ell+2}}k_1. \qquad \text{(C15)}$$

Finally, for resonant amplitude problems we will require c_{13} from $\mathcal{R}_1 = c_{13}\mathcal{R}_3 + c_{14}\mathcal{R}_4$. We see that in the near-field region $M \ll r \ll \omega^{-1}$, $\mathcal{R}_1$ is dominated by the growing-outward ($r^{\ell+2}$) solution while $\mathcal{R}_3$ and $\mathcal{R}_4$ are both dominated by the growing-inward ($r^{1-\ell}$) solution. Therefore the ratio $c_{13} : c_{14}$ can be obtained by forcing the leading terms inward (i.e. coefficients of $\propto r^{1-\ell}$) to cancel. This is

$$c_{13} = -\frac{k_4}{k_3}c_{14} = \mathrm{i}\frac{k_4\aleph}{2\omega k_3} = \mathrm{i}^{-\ell+1}\frac{(2\ell + 1)!}{(\ell + 2)!}(2\omega)^{1-\ell}k_1. \quad \text{(C16)}$$